Atmos. Chem. Phys., 16, 1331–1352, 2016
www.atmos-chem-phys.net/16/1331/2016/
doi:10.5194/acp-16-1331-2016

Atmospheric Chemistry and Physics Open Access EGU

On the long-term impact of emissions from central European cities on regional air quality

P. Huszar, M. Belda, and T. Halenka

Department of Atmospheric Physics, Faculty of Mathematics and Physics, Charles University, Prague, V Holešovičkách 2, 180 00 Prague 8, Czech Republic

Correspondence to: P. Huszar (peter.huszar@mff.cuni.cz)

Received: 20 October 2015 – Published in Atmos. Chem. Phys. Discuss.: 16 November 2015
Revised: 18 January 2016 – Accepted: 18 January 2016 – Published: 8 February 2016

Abstract. For the purpose of qualifying and quantifying the impact of urban emission from Central European cities on the present-day regional air quality, the regional climate model RegCM4.2 was coupled with the chemistry transport model CAMx, including two-way interactions. A series of simulations was carried out for the 2001–2010 period either with all urban emissions included (base case) or without considering urban emissions. Further, the sensitivity of ozone production to urban emissions was examined by performing reduction experiments with −20 % emission perturbation of NO_x and/or non-methane volatile organic compounds (NMVOC).

The modeling system's air quality related outputs were evaluated using AirBase, and EMEP surface measurements showed reasonable reproduction of the monthly variation for ozone (O_3), but the annual cycle of nitrogen dioxide (NO_2) and sulfur dioxide (SO_2) is more biased. In terms of hourly correlations, values achieved for ozone and NO_2 are 0.5–0.8 and 0.4–0.6, but SO_2 is poorly or not correlated at all with measurements (r around 0.2–0.5). The modeled fine particulates ($PM_{2.5}$) are usually underestimated, especially in winter, mainly due to underestimation of nitrates and carbonaceous aerosols.

European air quality measures were chosen as metrics describing the cities emission impact on regional air pollution. Due to urban emissions, significant ozone titration occurs over cities while over rural areas remote from cities, ozone production is modeled, mainly in terms of number of exceedances and accumulated exceedances over the threshold of 40 ppbv. Urban NO_x, SO_2 and $PM_{2.5}$ emissions also significantly contribute to concentrations in the cities themselves (up to 50–70 % for NO_x and SO_2, and up to 60 % for $PM_{2.5}$), but the contribution is large over rural areas as well (10–20 %). Although air pollution over cities is largely determined by the local urban emissions, considerable (often a few tens of %) fraction of the concentration is attributable to other sources from rural areas and minor cities. For the case of Prague (Czech Republic capital), it is further shown that the inter-urban interference between large cities does not play an important role which means that the impact on a chosen city of emissions from all other large cities is very small. At last, it is shown that to achieve significant ozone reduction over cities in central Europe, the emission control strategies have to focus on the reduction of NMVOC, as reducing NO_x (due to suppressed titration) often leads to increased O_3. The influence over rural areas is however always in favor of improved air quality, i.e. both NO_x and/or NMVOC reduction ends up in decreased ozone pollution, mainly in terms of exceedances.

1 Introduction

Cities have a significant environmental impact that follows primarily two pathways. They emit a large amount of gaseous species and aerosols into the air, having direct impact on the composition and chemistry of the atmosphere (Timothy and Lawrence, 2009) and harmful effect on the population (Gurjar et al., 2010). Secondly, having specific mechanical, radiative, thermal, and hydraulic properties, urban surfaces af-

fect meteorological conditions and therefore the climate (Lee et al., 2011; Huszar et al., 2014).

The first pathway has an indirect impact on the meteorology and climate as well. Certain gases and aerosols interact with radiation in the atmosphere, modifying the radiative and consequently the thermal balance resulting in temperature changes. Aerosols further interact with the clouds, changing their micro-physical and optical properties (Seinfeld and Pandis, 1998).

Emission from cities encompass the oxides of nitrogen (NO_x), that are produced mainly during fossil fuel combustion in road transportation and energy production. Carbon monoxide (CO) is a product of incomplete combustion and is dominantly emitted in African and Asian cities reflecting the older-than-average technologies used (Streets and Waldhoff, 2000). Non-methane volatile organic compounds (NMVOCs) are products of road transport and solvents use in North American and European cities; however in Africa and Asia, they originate mainly from domestic combustion (Denier van der Gon et al., 2010). SO_2 emissions are released mainly due to energy production and industry and they are relatively low in European cities.

Emissions of NO_x and VOC are predominantly affecting photochemistry and depending on their ratio, the photochemical regime in and around cities is either NO_x-controlled or VOC-controlled (Xue et al., 2014). When the concentrations of NO_x are much higher than of VOCs (NO_x-saturated case), the ozone (O_3) formation is controlled by the changes of VOCs: ozone increases with increasing VOCs while if NO_x increases, ozone decreases by titration. This regime is called VOC-controlled. On the other hand when VOCs / NO_x ratio is high, ozone production depends on the change of nitrogen oxides: with increasing NO_x concentration ozone increases as well and a NO_x-controlled regime occurs (Sillman, 1999). The ratio NO_x / VOC is usually high in North-American agglomerations, many eastern Asian cities and in European agglomerations like Athens, Paris, Milan or Berlin as well and ozone is usually titrated over these cities (Beekmann and Vautard, 2010). However, according to actual meteorological conditions, pollution from cities can be transported over large distances where the aged plume from the city mixes with additional VOC sources and can become NO_x sensitive leading to ozone production (Beekmann and Derognat, 2003). The overall effect of city emissions on ozone production and/or destruction can further depend on model's resolution. Thunis et al. (2007), analyzing Berlin, Milan, Paris and Prague found that while models with large spatial step usually predict ozone production due to emissions from cities, high-resolution modeling studies attribute VOC-controlled regime to cities that leads to ozone destruction.

Emissions of gaseous pollutants from cities can further perturb the aerosol burden. Sulfur dioxide, nitrogen (di)oxide and ammonia emissions lead, in presence of water vapor, to the formation of secondary inorganic aerosols: ammonium-sulfate-nitrate particles (Martin et al., 2004). The primary precursor for sulfate aerosol (PSO_4) formation is sulfur dioxide. Barth and Church (1999) investigated the sulfate formation due to SO_2 originating from Mexico City and cities from southeastern China, still the largest SO_2 emitter regions nowadays. They found significant perturbation of the global sulfate aerosol burden due to these two regions and cities located therein. NO_x emissions do not affect only photochemistry (and the consequent ozone formation/destruction) but also the formation of nitrate aerosol (PNO_3). If the meteorological conditions are favorable, nitrate oxide emissions from cities can enhance background nitrate aerosol levels significantly (Lin et al., 2010). Emissions of ammonia (NH_3) from cities are an efficient contributor to formation of sulfate and nitrate aerosol (by forming ammonium-sulfates and ammonium-nitrates) and its importance in connection with cities emissions are studied recently by many (Behera and Sharma, 2010, and references therein). Generally, the thermodynamic system of ammonium-sulfate-nitrate-water solution is rather complicated and its equilibrium state is highly dependent on the initial ratio of $SO_2 : NO_x : NH_3$ given by their emissions, and the governing meteorological conditions (Martin et al., 2004), thus the contribution of different cities to these particles can be very variable.

Finally, organic gaseous material (volatile, intermediate- and semi-volatile VOC) released from cities can contribute to formation of secondary organic aerosols and significantly enhance the total aerosol burden in urban, as well as the downwind environment, as showed by Paredes-Miranda et al. (2009), Hodzic et al. (2010) and Zhang et al. (2015).

Numerous studies were dealing with the impact of emissions from cities on air quality over local, regional and even global scale. Many of them were based on measurements within and outside of the urban plumes from particular cities (Freney et al., 2014; Lin et al., 1996; Gaffney et al., 1999; Molina et al., 2010; Kuhn et al., 2010; Wang et al., 2006). There has also been model-based efforts to estimate the cities fingerprint on the atmospheric chemistry across multiple scales: on a global scale, Lawrence et al. (2007), Butler and Lawrence (2009), Folberth et al. (2010) and Stock et al. (2013) gave estimates on the city emissions impact on the surrounding environment. On regional scales, many studies focused on European urban centers, especially those in the Mediterranean region (e.g. Im et al., 2011a, b; Escudero et al., 2014; Finardi et al., 2014), but also covering London and the Ruhr area (Hodnebrog et al., 2011), or Paris (Skyllakou et al., 2014; Markakis et al., 2015). The importance of multi-model modeling approach for investigating the megacities impact on air quality and climate was analyzed in detail by Baklanov et al. (2010) in the framework of the European FP7 project MEGAPOLI. Within another European project, FP7 project CITYZEN, Im and Kanakidou (2012) investigated the impact of emissions from eastern Mediterranean megacities, Athens and Istanbul.

Here we present a study that is inspired by a wider effort to describe quantitatively the urban/climate/air quality inter-

actions over the target area of central Europe. Previously, Huszar et al. (2014) presented the impact of urban landsurface forcing on climate. Here, we link it to this study and look at a further aspect of the urban impact on environment: we aim to provide a chemistry transport model-based estimate of the long-term impact of emissions from cities in central Europe on the regional air quality. The study brings four novelties: (1) the above listed studies over Europe focused either on the region of Mediterranean, which encounters dry warm climate, and/or on large megacities only (London, Paris, Istanbul, Athens). In contrary, our target region is central Europe with different climate (temperate maritime to continental) and without any megacity. (2) Previously, model based estimates of urban emission impact over Europe considered relatively short time periods (1–2 months) often separately for winter and summer seasons (e.g. Im et al., 2011a; Im and Kanakidou, 2012; Finardi et al., 2014). These periods are however short to eliminate the potential influence of specific meteorological conditions during those time periods. Therefore, we have proposed to conduct continuous, 10-year long simulations which decreases the uncertainty originating in the driving meteorological conditions. This choice was preferred also by Katragkou et al. (2010) and Zanis et al. (2011) or Markakis et al. (2015). (3) Most of the above-listed regional studies focused on only one or two megacities (and their impact). Here we consider all large cities within the region in focus. This is an important step, as the combined impact of emissions from all cities may, due to chemical nonlinearities, significantly differ from the cumulative impact evaluated separately for each city. (4) Our study evaluates the impact on policy-relevant metrics that include also exceedances above a threshold, instead of evaluating simply seasonal averages that often lack information on extreme pollution.

The study has two main goals: (1) to evaluate the present-day contribution of city emissions to the regional air pollution over central Europe. (2) To calculate the potential impact of mitigation strategies by testing the regional fingerprint of urban emissions reductions. The possible climate impact of the presented urban-induced chemical perturbation of the atmosphere will be addressed as well in a future paper. Within the first goal, the study tries to answer two questions: (a) what is the contribution of urban emissions to the air quality over rural areas further from cities, (b) to what extent is the urban air quality influenced by non-urban emissions? Regarding the second goal, the question asked is which urban emission reductions are the most effective in controlling regional-scale ozone pollution.

The impact will be evaluated in terms of surface concentrations and exceedances of key gaseous pollutants (O_3, NO_2, SO_2) and fine aerosol (size $< 2.5\,\mu m$, $PM_{2.5}$).

2 Emissions

Emissions used in the study are the TNO emissions prepared for 2005 in the framework of the FP 7 MEGAPOLI project (Kuenen et al., 2010). This high-resolution ($1/8^\circ$ longitude $\times$ $1/16^\circ$ latitude, roughly 7 km $\times$ 7 km) European emission database provides annual emissions estimates for NO_x, SO_2, NMVOC, CH_4, NH_3, CO and primary PM_{10} and $PM_{2.5}$ in 10 source sectors.

For the purpose of calculating the impact of urban emissions, emission mask had to be built for selected cities. These were built according to the administrative borders of the particular city in combination with the subgrid urban land-surface data used in Huszar et al. (2014), originally extracted from the Corine2006 database (EEA, 2012). The selection of certain cities, in general, comprises cities considered to be large within the particular region. As such we chose the threshold of 500 000 inhabitants representing a "large" city. This threshold was reduced to 200 000 inhabitants over selected regions (Czech Republic, Slovakia, Hungary, Romania, partly Poland, Austria, Italy). Figure 1 presents the distribution of the annual emissions over selected cities for the main pollutants: CO, NMVOC, NO_x, NH_3, SO_2 and $PM_{2.5}$. It clearly reveals the emission density differences between the urban centers and suburban areas and that the emissions are mostly comprised of CO, NO_x and NMVOC, which can reach 500, 100 and 100 $Mg\,km^{-2}\,yr^{-1}$, respectively, especially in urban centers.

Figure 2 plots the absolute annual emissions for the whole domain, for all the cities and for six selected cities (namely, Vienna, Budapest, Berlin, Prague, Munich, Warsaw). The plot shows that in most of the sectors, urban emissions form roughly 10 % of all emissions, while they cover slightly more than 3.5 % of the area of the focused region. The sector to which they contribute less is the agriculture where they emit less than 0.5 % of all emissions.

In general, road transportation is the sector contributing most to urban emissions, followed by non-industrial combustion in Central Europe. However, large differences are identified between cities. While emissions from sector SNAP 8 that include ship and airport traffic are generally small, in selected cities with major international airports or intense vessel traffic (on rivers), these can be of comparable magnitude with the road transportation (e.g. Munich), or even exceed road traffic (Vienna).

The most contributing substance to city emissions is carbon monoxide with an approximately 56 % contribution (in mass units) on average, followed by NO_x and NMVOC both with around 14 %. SO_2 makes 12 % of all the city emissions on average, being somewhat higher in eastern European urban centers (almost 20 % in Budapest, and 18 % in Warsaw).

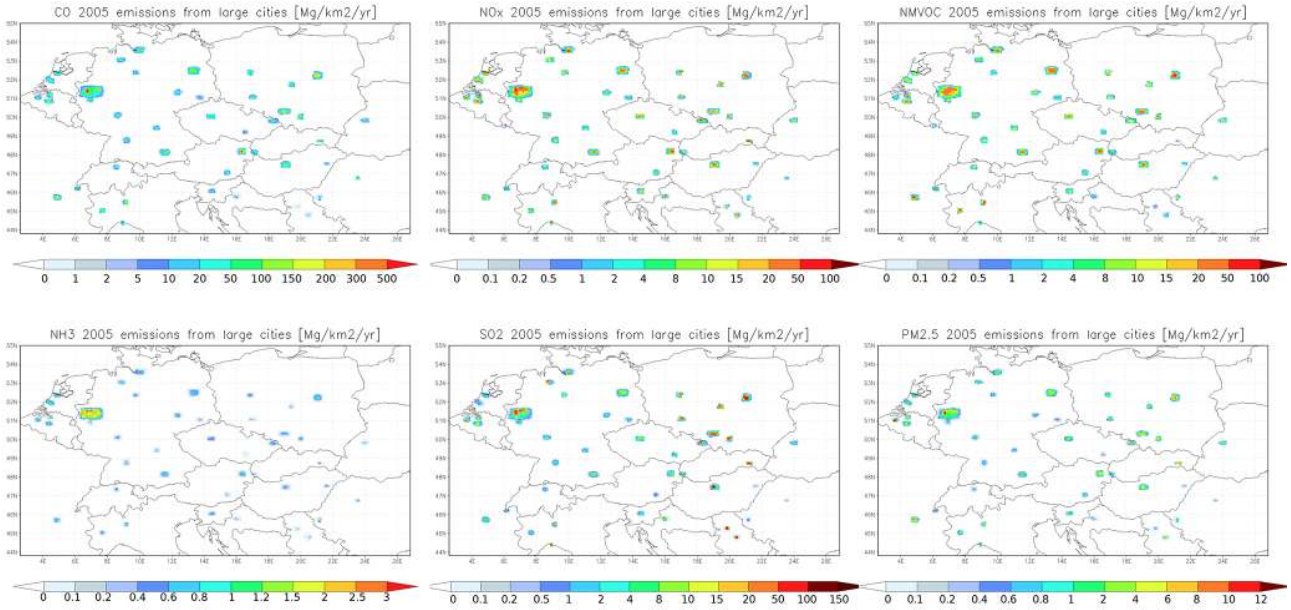

Figure 1. Annual emissions from the cities considered in the study based on the TNO MEGAPOLI 2005 emissions as $\mathrm{Mg\,km^{-2}\,yr^{-1}}$ for CO, NO_x, NMVOC, NH_3, SO_2 and $PM_{2.5}$.

3 Models and experimental design

3.1 The regional climate model RegCM4.2

As a meteorological driver, we used the regional climate model RegCM version 4.2 (hereafter referred to as RegCM4.2) developed by The International Centre for Theoretical Physics. Although the up-to-date version of RegCM is 4.5 (June 2015), the development of the modeling tools for this study started earlier when the newest version was 4.2. RegCM4.2 and its evolution from RegCM3 is fully described by Giorgi et al. (2012). Its dynamical core is based on the hydrostatic version of the NCAR-PSU Mesoscale Model version 5 (MM5) (Grell et al., 1994). The radiation is solved within the Community Climate Model version 3 (CCM3) (Kiehl et al., 1996). The large-scale precipitation and cloud processes are calculated following Pal et al. (2000) and for convection parameterization we use the Grell scheme (Grell, 1993) using the Fritsch and Chappell (1980) closure assumption in this study. RegCM4.2 includes two land-surface models: Biosphere–Atmosphere Transfer Scheme (BATS) originally developed by Dickinson et al. (1993) and the CLM3.5 model (Oleson et al., 2008). In this study, the BATS scheme is activated. The single layer urban canopy model coupled to RegCM4.2 introduced by Huszar et al. (2014) was not applied assuming that the urban-meteorological influence on the emissions impact will be minor and furthermore, to meet the computational demand of long climate simulations.

3.2 The chemistry transport model CAMx

The chemistry simulations were carried out with the chemistry transport model CAMx (version 5.4). CAMx is a Eulerian photochemical dispersion model developed by ENVIRON Int. Corp. (http://www.camx.com). CAMx includes the options of two-way grid nesting, multiple gas phase chemistry mechanism options (CB-IV, CBV, CBVI, SAPRC99), evolving multi-sectional or static two mode particle size treatments, wet deposition of gases and particles, plume-in-grid (PiG) module for sub-grid treatment of selected point sources, Ozone and Particulate Source Apportionment Technology, mass conservative and consistent transport numerics and parallel processing. The ISORROPIA thermodynamic equilibrium model (Nenes et al., 1998) is implemented in CAMx to calculate the composition and phase state of an ammonia-sulfate-nitrate-chloride-sodium-water inorganic aerosol system in equilibrium with gas phase precursors. A detailed description of the model (the version used here) can be found at http://www.camx.com/files/camxusersguide_v5-40.pdf.

3.3 The coupled model RegCMCAMx4

To achieve the goals of the study, a coupled system was designed consisting of RegCM4.2 and CAMx (denoted RegCMCAMx4) following the technique of online access coupling defined by Baklanov (2010). It represents an interactive two-way coupled modeling framework where chemistry is driven by the climate model and the calculated con-

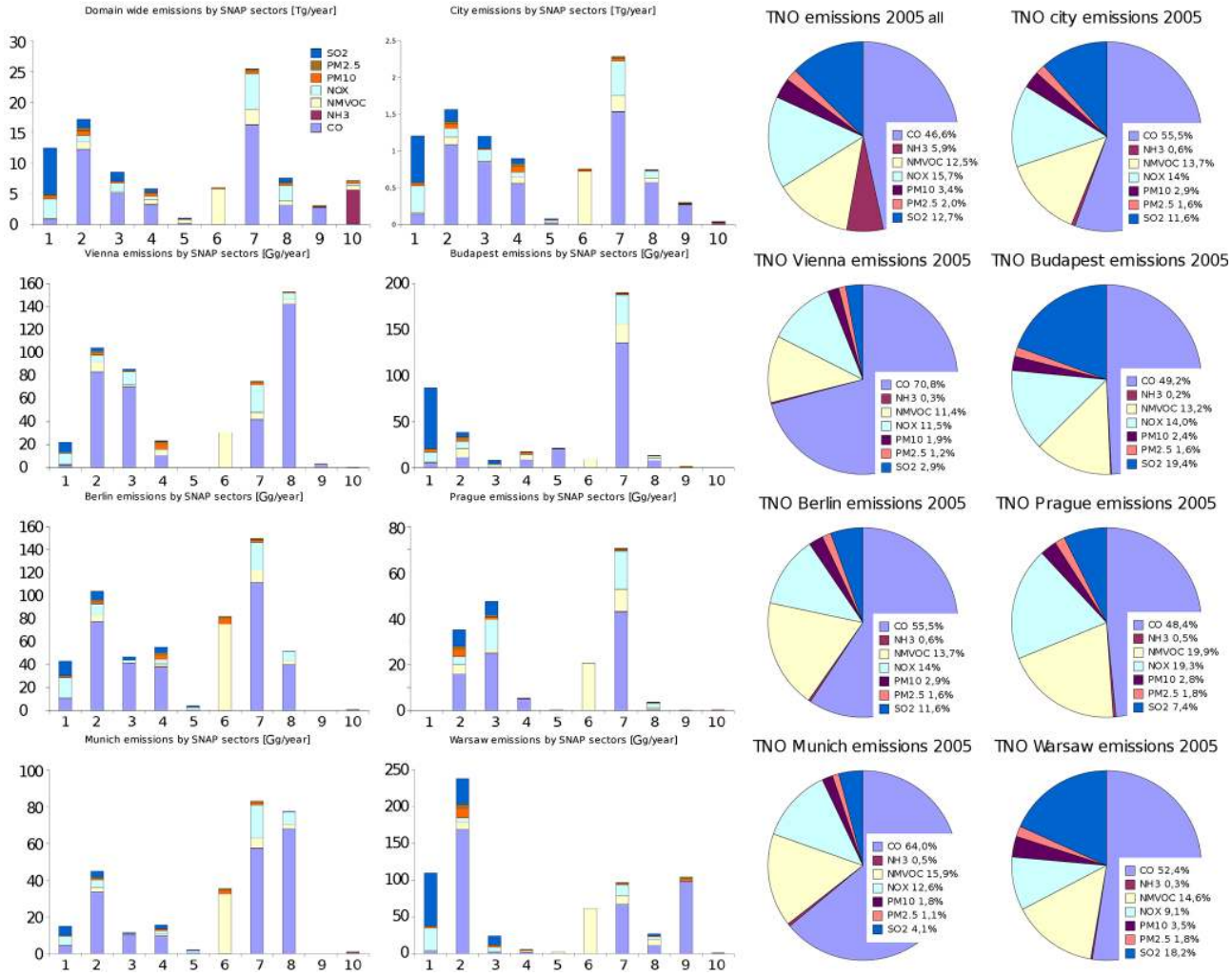

Figure 2. First two columns: annual emissions (2005) per sector for the entire domain in Tg yr^{-1}, for all the cities in Tg yr^{-1} and for six selected cities from the domain in Gg yr^{-1}. Right two columns: the same as the first one, but for the relative contribution of individual pollutants in %.

centrations of the radiatively active gases and aerosols are fed back to the climate model's radiation code.

RegCMCAMx4 is a more advanced version of the original RegCMCAMx couple described by Huszar et al. (2012). The update interval for the meteorology from RegCM remained at 1 h which is sufficient (Grell and Baklanov, 2011). However, the original update interval for the species in the radiation code of 6 h was too coarse for describing the diurnal species evolution, therefore it has been reduced to 1 h as well. The original RegCMCAMx considered only the direct effect of sulfates and primary organic and black carbon. RegCMCAMx4 introduces the indirect effect of secondary inorganic aerosols (both sulfates and nitrates). For sulfates, it follows the work of Giorgi et al. (2003) where the cloud droplet concentration and effective droplet radius is modified according to the aerosol concentration. For nitrates both direct and indirect radiative effects are computed with the same method as for sulfates but with slightly modified optical properties following the works of McMeeking et al. (2005) and Wang et al. (2010).

RegCMCAMx4 further replaces the O'Brien (1970) method for calculating the coefficients of vertical turbulent diffusion (which is required by CAMx) with the newer Byun (1999) scheme (as used in CMAQ model), which provides better agreement of model results with measurements, as shown by Eben et al. (2005) in a CAMx application over the same region and at similar horizontal resolution like in this study.

The added value of using an online coupled climate–chemistry modeling system is the possibility to calculate radiative feedbacks and impacts on temperature (and climate in general). We also assumed, based on previous validation studies involving RegCM and CAMx that the capability of these models reproducing the state of the atmosphere (both

meteorology and chemistry) will not change significantly if coupling them online with respect to the case when they are coupled offline (e.g. Huszar et al., 2012).

3.4 Experimental set-up

The period of 2001–2010 was chosen to analyze the present-day impact of urban emissions on the air quality over central Europe. Calculation with RegCMCAMx4 were carried out on 10 km × 10 km horizontal resolution domain centered over Prague, Czech republic of 160 × 120 × 24 (in x, y, and z direction) gridboxes for the climate model up to 50 hPa, while the chemistry model was integrated only on the lowermost 16 levels (approximately up to 300 hPa or 9000 m). The integration time step for the climate model was 30 s and 10 min for the chemistry model.

The ERA Interim reanalysis (Simmons et al., 2010) was chosen as driving meteorological conditions while for the chemical model, chemical boundary conditions (CBC) were taken from a similar 10-year run performed by RegCM-CAMx4 over a larger, 30 km × 30 km domain covering the whole of Europe.

As already mentioned, the TNO 2005 emissions were chosen to cover the studied period. Over the focused region, their resolution is about 7 km × 7 km, which is sufficient for a 10 km × 10 km computational grid. TNO are sector based annual emission data which were first regridded into the model grid. Than for each sector, specific temporal disaggregation factors and NMVOC speciation profiles were used to decompose the annual sums into hourly emissions following the inventory (Winiwarter and Zueger, 1996). The temporal profiles they provide were compiled to describe typical central European human activity profiles regarding transport, combustion, production etc. Biogenic emission of isoprene and monoterpenes were calculated following Guenther et al. (1993).

A number of experiments was carried out to examine the effect of city emissions on the regional air quality. These are summarized in Table 1. The total impact of all city emissions is evaluated as the difference between experiments 05BASE and 05ZERO (the "05" means that the 2005 emission were used). We were also interested in the impact the emissions from all other cities have on a selected city. To achieve this goal, we performed a run where all city emissions are removed except those from Prague. Apart from the total impact, it is also of interest to see how the individual species emitted contribute to the overall impact. We therefore evaluate also the partial impact of major gaseous pollutants, namely NO_x, NMVOC. As the interest of policy makers is to estimate the consequences of possible emission reduction in cities, we propose to evaluate this partial impact in a framework of a sensitivity test where the emissions of the above-mentioned pollutants will be reduced by 20 %. For the sensitivity runs, no radiative feedbacks were calculated and the same meteorological conditions were thus used as a driver for these simulations. The assumption made here was that the main driver for the air quality changes are emissions, as the meteorological impact of the online coupled ozone and aerosols are expected to be small, having small feedback to the chemistry.

4 Results

4.1 Model validation

In order to justify the model's applicability for the presented goal, a detailed quantitative validation is provided for surface concentrations of O_3, NO_2, SO_2 and $PM_{2.5}$. We also included a minimal validation of the meteorological results: the near surface temperature is compared with the European EOBS climate data set (Haylock et al., 2008) that is currently extended until 2014. A detailed validation for the meteorological output is planned in a follow-up study, which intends to present the meteorological feedbacks of the presented chemical perturbation induced by urban emissions. Figure 3 presents the comparison of model seasonal near surface temperatures averaged over the 2001–2010 period with the E-OBS gridded data set. It indicates a negative model bias, which is highest in spring (around −1 to −2 K over large areas) and lowest in summer (0 to −1.5 K). This is attributable to overestimated cloudiness in RegCM, as already concluded by Huszar et al. (2014), who used the same model and set-up. Over mountainous areas like the Alps, southeastern Carpathians, biases reach values from −5 to 5 K, however, this is most probably related to coarse model representation of specific terrain features (valleys, ridges etc.) that highly determine the surface temperatures. A striking feature is the overestimation of temperature on eastern edge of the domain. As the boundary-close cells of the domain are strongly influenced with the boundary conditions, this may indicate that the reanalysis used (ERA Interim) is somewhat warmer than the gridded observational data.

For the chemical validation, the AirBase version 8 data (http://www.eea.europa.eu/data-and-maps/data/airbase-the-european-air-quality-database-8) provided by the European Environmental Agency, are used. We selected only rural background stations which are more consistent with the model-provided value that represents a 10 km × 10 km average. Further the stations ale filtered to exclude high-elevation stations (above 2000 m). In the end, 328 stations for O_3, 280 for NO_2, 200 for SO_2 and 53 for $PM_{2.5}$ were selected for comparison with model results. For the gaseous pollutants, hourly, daily and monthly averages are considered while for aerosols only daily and monthly data are considered. The validation is done separately for winter (DJF), summer (JJA) months and for the whole year. The statistical measures evaluated were the correlation coefficient (r), root mean square error (RMSE), normalized mean square error (NMSE), the ratio of standard deviations

Table 1. Summary of the conducted experiments including the experiment name, the time period, the emissions considered and whether radiative feedbacks on meteorology are considered.

Experiment	Period	Emissions	Radiative feedbacks
05ZERO	2001–2010	All except cities	yes
05BASE	2001–2010	All	yes
05ZEROPRAGUE	2001–2010	Urban emission only from Prague	yes
0580NO_x	2005–2009	80 % urban NO_x emissions	no
0580NMVOC	2005–2009	80 % urban NMVOC emissions	no
0580N80 V	2005–2009	80 % urban NO_x and NMVOC emissions	no

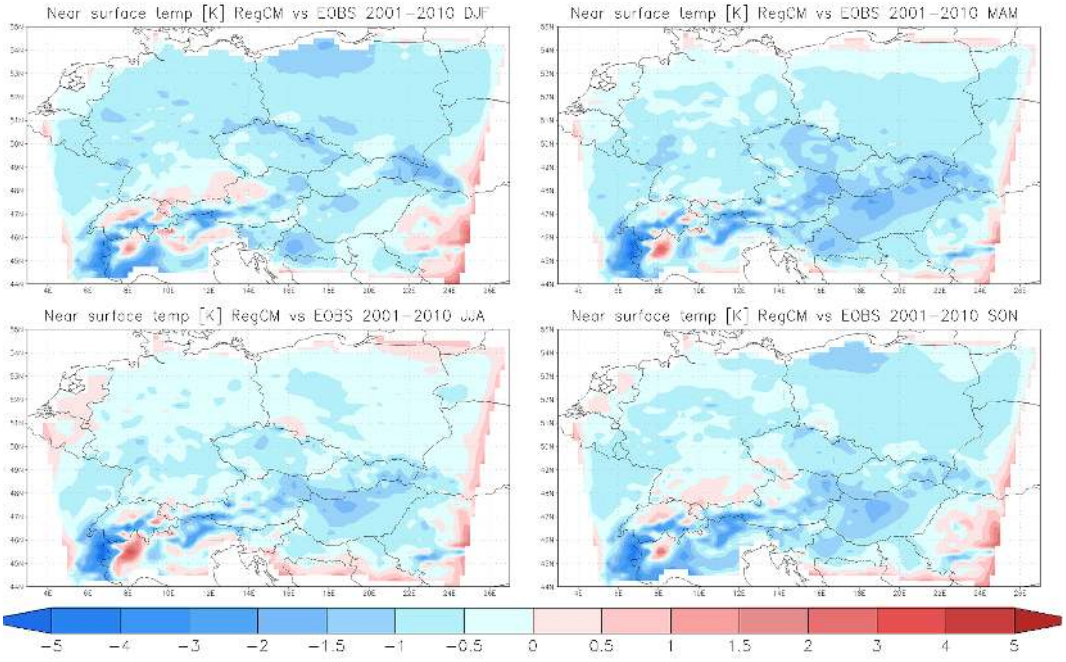

Figure 3. Comparison of the 2001–2010 seasonal mean near surface temperatures from the base (05BASE) experiment with EOBS measurements for winter (DJF), spring (MAM), summer (JJA) and autumn (SON) in K.

(σ_r, calculated as $\sigma_{observation}$ divided by σ_{model}) and fractional bias (FB), as defined by Borrego et al. (2008) and adopted by Juda-Rezler et al. (2012). They identified these metrics as the most important in assessing air quality model accuracy. Choosing these metrics further eases the comparison of the RegCMCAMx4 model performance with its former version presented in Huszar et al. (2012) who applied the same metrics. The experiment 05BASE gave the base for the validation.

The above-mentioned statistical measures are collected in Table 2 for O_3, NO_2, SO_2 and $PM_{2.5}$. 3-3-3 columns are dedicated for hourly, daily and monthly data averaged over the whole year, DJF and JJA, respectively.

The average monthly and hourly cycles for DJF and JJA were selected, which provide a measure of the model's ability to capture the basic chemical climatology of key-species concentrations. Figure 4 plots the average monthly variation (left column) of the gaseous species O_3, NO_2 and SO_2. The middle and right column provide the average diurnal cycle of these species for DJF and JJA, respectively.

Further, the monthly mean values of $PM_{2.5}$ and its major components were compared to observations (Fig. 5) distinguishing between DJF and JJA. For PSO_4 and PNO_3, measurements from the already mentioned AirBase database were used. For carbonaceous aerosol, the monthly data from the BC/OC measurement campaign data described by Yttri et al. (2007) covering July 2002–June 2003 were used with the assumption that the basic climatology of these data is similar to the 2001–2010 average. These measurements considered BC/OC from PM_{10} aerosol (size $< 10\,\mu m$), our model (CAMx) that uses a two bin approach (fine and coarse particles), calculates them as fine particles (size $< 2.5\,\mu m$). We applied the factor of 0.8 to the measured values to estimate the $PM_{2.5}$ fraction. This value is compiled from Chen

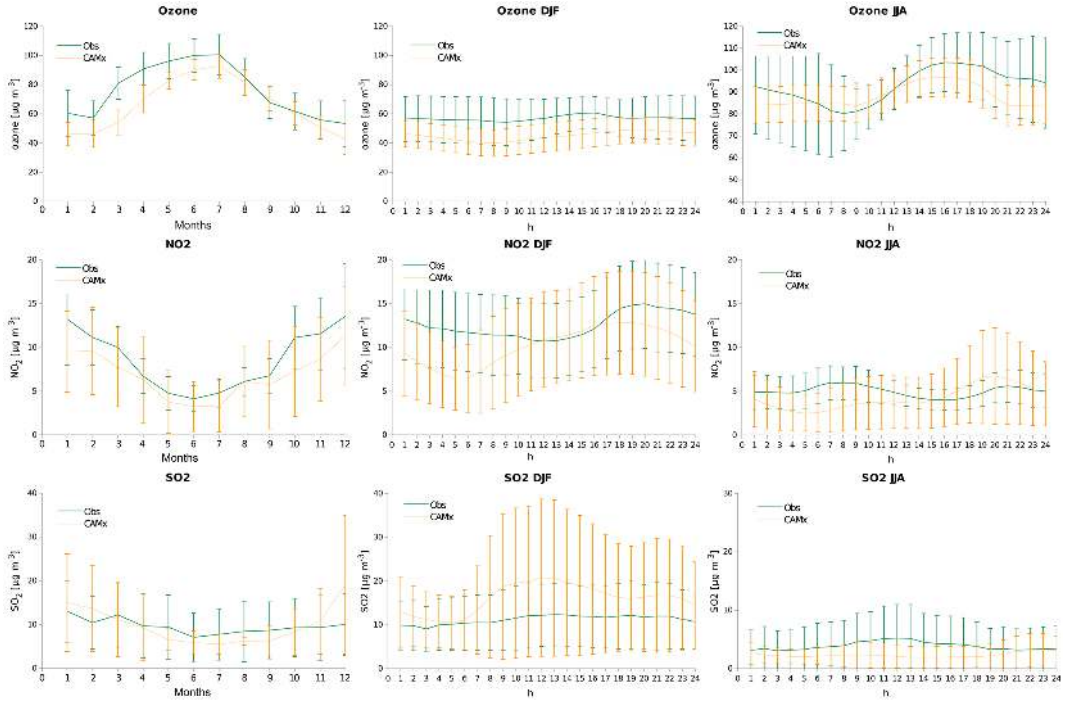

Figure 4. Left column: comparison of the 2001–2010 mean monthly variation of O_3, NO_2 and SO_2 averaged over all stations with vertical error bars indicating the standard deviation of the average. Middle column: comparison of the 2001–2010 DJF mean diurnal variation for the same species with error bars indicating the standard deviation of the average. Right column: same as middle column but for summer months (JJA).

et al. (1997), Offenberg and Baker (2000) and Samara et al. (2014) as an average of different seasons and character of the measurement site (cold vs. warm season and urban vs. rural).

We assessed the model bias further for urban stations as well, although it is well accepted that these stations are not suitable for standard chemistry transport model evaluation (at such resolution as in this study). We selected 10 urban background stations for Berlin, Budapest, Frankfurt, Katowice, Ljubljana, Milan, Munich, Prague, Vienna and Warsaw. The same statistical metrics were chosen as above but only for hourly (daily) averages for gases (particle matter). The results are collected in Table 3.

4.1.1 Ozone

The correlations of modeled ozone data with measurements are highest for the monthly means reaching 0.77 when considering the whole period. It is generally lower in DJF than during JJA and decreases for shorter averaging periods. For the hourly means, it is about 0.57 for the whole period, and about 0.41 and 0.53 for DJF and JJA. Relatively high RMSE and NMSE values are modeled for the hourly values and get smaller for longer averaging period (around $17\,\mu g\,m^{-3}$ for the monthly means). The ratios of standard deviation are slightly higher than 1 indicating that the measured ozone values have higher variability than the modeled ones. In terms of fractional bias, the model underestimates ozone for both DJF and JJA (FB being around -16 and $-2\,\%$) giving an overall underestimation of FB $= -4.3\,\%$ for the whole period.

The negative ozone bias is clearly seen in terms of the monthly means and is highest during early spring ($-20\,\mu g\,m^{-3}$) and reaching almost zero during August, September and October. On an hourly basis, the model is always negatively biased in DJF (by 10–15 $\mu g\,m^{-3}$) showing minimum diurnal variations (in accordance with the measurements). During JJA, the model reasonably captures the timing of the ozone daily maximum values but underestimates the daily amplitude by giving smaller daytime peak values by almost $20\,\mu g\,m^{-3}$.

The correlations for individual cities are lower in general but the RMSE are of similar value. FBs indicate a slight overestimation in JJA, in contrary with the rural station values. The DJF negative bias is stronger for urban stations than for their rural counterparts.

4.1.2 Nitrogen dioxide

The modeled NO_2 values are less correlated with the measured ones than in the case of ozone. Again, they are highest for the monthly means (0.68, 0.59 and 0.62 for the whole period, for DJF and JJA months, respectively). The RMSE values are lower than for O_3, being highest for DJF and for the

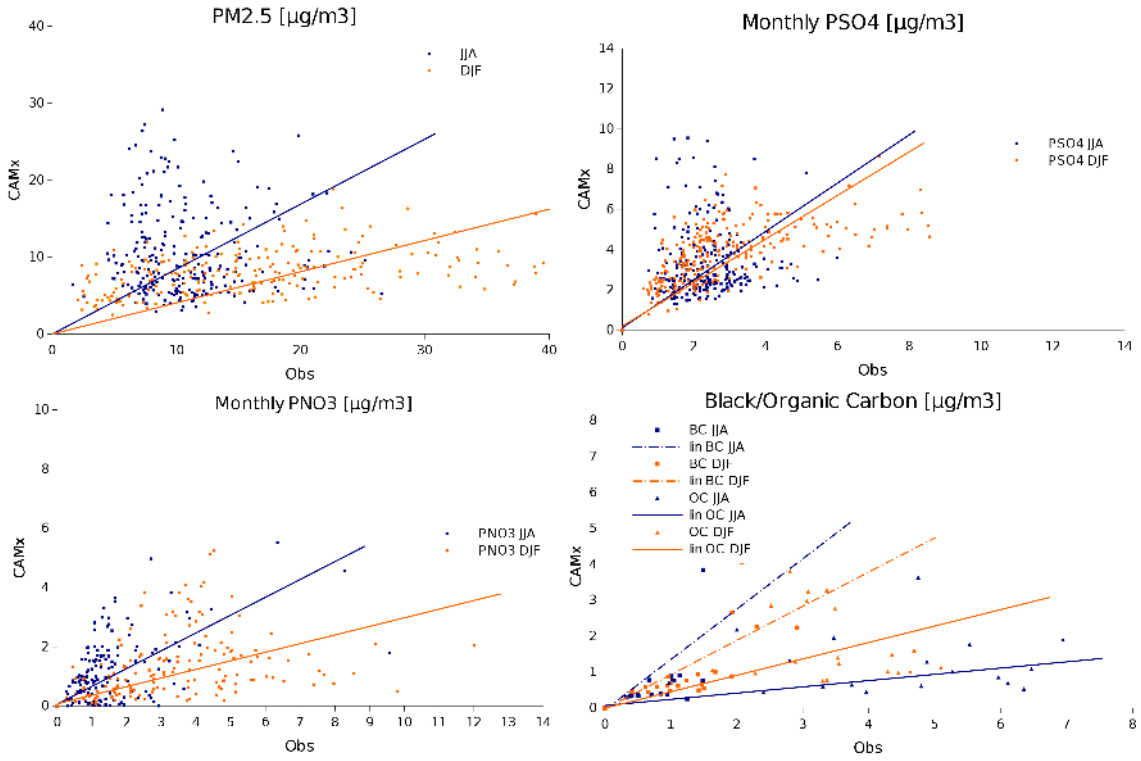

Figure 5. Comparison of monthly values of $PM_{2.5}$ and its major components (sulfate-, nitrate aerosol, black and organic carbon) for DJF (orange) and JJA (dark blue) months. For carbonaceous aerosol, square stands for BC and triangle for OC. Linear trend lines are also shown.

hourly means (around 19 µg m^{-3}). The observation-model agreement is in general best for JJA. However, during JJA, the model exhibits much larger standard deviation than the measured values, while during DJF, the ratio of standard deviations is close to 1. In general, the model tends to underestimate both DJF and JJA NO_2 values with FB values around −14.8, −23.7 and −10.5 % for all the months, for DJF and JJA, respectively. This is also well described by the average monthly and diurnal variation plots (Fig. 4, middle row): the DJF NO_2 values are underestimated by up to 5 µg m^{-3} but a fair agreement is modeled during late spring to early autumn months with only a slight underestimation around 1–2 µg m^{-3}.

The diurnal course for DJF is captured in the model as well, but it peaks around 18:00 UTC compared to 20:00 UTC in observations. The diurnal amplitude is of comparable magnitude due to both maximum and minimum values lower in model than in observations. Especially the nighttime NO_2 values are underestimated during DJF (by more than 5 µg m^{-3}). In JJA, the observations reveal two peaks, in the morning and early evening hours, but the model reproduces (although poorly) only the evening peak with an overestimation around 2 µg m^{-3}.

Similarly to ozone, the observation-model correlation for individual cities is much smaller, or there is no correlation at all. The model remains negatively biased but it is highest for JJA. The variability in urban stations is highly underestimated, in opposite to the rural stations above.

4.1.3 Sulfur dioxide

The model results of SO_2 are, in general, characterized by a low correlation with measurements, especially for the hourly averages. Highest correlations are achieved for monthly values (over $r = 0.5$). The RMSE values are highest for the hourly values and lowest for the monthly ones indicating a better model-observation agreement in terms of monthly means. The standard deviation of the modeled values is overestimated in DJF, however in JJA, the observed standard deviations are more than two times higher than the modeled ones. The FB values indicate that the DJF SO_2 values are overestimated in DJF and underestimated in JJA (−50 and 55 %, respectively).

The overestimation of SO_2 in DJF is apparent from the average monthly and diurnal cycle in DJF (Fig. 4, bottom left). The model predicts much larger concentrations than the observed ones especially in December, and, in terms of the hourly variation, during midday. During JJA, SO_2 is underestimated by 2–3 µg m^{-3}, especially during noon hours.

From an urban station perspective, the model is very poorly correlated with measurements (correlations not exceeding 0.4) and the values are strongly overestimated (often

Table 2. Comparison of model data with measurements: evaluation of the correlation coefficient (r), root mean square error (RMSE; in $\mu g\,m^{-3}$), normalized mean square error (NMSE), the ratio of standard deviations (σ_r) and fractional bias (FB; in %) for hourly, daily and monthly averages for winter (DJF) and summer (JJA) months and for the whole year ("annual") for pollutants O_3, NO_2, SO_2 and $PM_{2.5}$. For $PM_{2.5}$, no hourly data were available.

		Hourly			Daily			Monthly		
		Annual	DJF	JJA	Annual	DJF	JJA	Annual	DJF	JJA
Ozone	r	0.569	0.408	0.533	0.671	0.485	0.621	0.770	0.610	0.700
	RMSE	32.073	28.880	33.903	25.207	24.586	24.245	18.411	17.253	16.392
	NMSE	0.301	0.510	0.196	0.185	0.369	0.100	0.097	0.182	0.045
	σ_r	1.174	1.167	1.303	1.063	1.184	1.067	1.072	1.327	1.095
	FB	−4.3	−16.4	−2.3	−4.3	−16.3	−2.3	−4.4	−16.1	−2.1
NO_2	r	0.451	0.409	0.342	0.547	0.466	0.464	0.683	0.590	0.618
	RMSE	15.940	19.073	13.190	12.745	15.871	10.042	8.906	10.746	7.245
	NMSE	1.282	1.005	1.925	0.816	0.697	1.116	0.403	0.320	0.592
	σ_r	0.839	1.004	0.639	0.854	1.039	0.612	0.870	1.053	0.633
	FB	−14.8	−23.7	−10.5	−14.8	−23.5	−10.4	−14.4	−21.3	−10.4
SO_2	r	0.305	0.292	0.255	0.397	0.361	0.363	0.579	0.532	0.492
	RMSE	15.086	27.155	9.730	11.346	21.694	7.648	12.409	14.950	5.787
	NMSE	6.436	6.683	8.531	2.822	2.102	5.244	7.065	7.515	2.956
	σ_r	0.670	0.749	2.517	0.645	0.747	2.406	0.641	0.721	2.362
	FB	20.0	51.1	−36.1	19.0	50.9	−35.9	19.7	49.9	−35.7
$PM_{2.5}$	r	–	–	–	0.374	0.409	0.313	0.419	0.458	0.376
	RMSE	–	–	–	21.209	30.675	15.488	15.871	22.805	9.891
	NMSE	–	–	–	2.825	4.948	1.695	1.578	2.836	0.725
	σ_r	–	–	–	1.886	3.396	0.447	1.783	3.690	0.492
	FB	–	–	–	−52.5	−92.6	18.3	−49.0	−90.2	16.2

by more than 100 % in terms of FB) in both JJA and DJF, in contrary to model performance evaluated for rural stations.

4.1.4 $PM_{2.5}$ and components

The modeled $PM_{2.5}$ values are low correlated with measurements and higher for monthly values and for DJF (up to $r = 0.45$). In terms of RMSE and NMSE, the model performs better during JJA, especially for the monthly means. In DJF, the standard deviation of the observed values is largely underestimated by the model, while in JJA, only half of the observed variability is predicted. $PM_{2.5}$ is largely underestimated in DJF (with around −90 % fractional bias) and slightly overestimated in JJA (FB = 17 %). This is further well seen on the monthly scatter plot in Fig. 5 (upper row, left). The DJF values (orange) do not exceed $20\,\mu g\,m^{-3}$ in DJF in the model, while they often reach $40\,\mu g\,m^{-3}$ in observations. In JJA, the range of values is similar, but the correlations are low, as already seen in Table 2.

The monthly scatter plots of individual components of the $PM_{2.5}$ aerosol are plotted in Fig. 5 as well. A relatively good agreement is achieved for PSO_4 during DJF with values ranging in both measurements and model up to $8\,\mu g\,m^{-3}$. However, sulfates are often over-predicted by the model in JJA. A different situation occurs for PNO_3, where the model exhibits a negative bias, especially for DJF, when values often above $6\,\mu g\,m^{-3}$ are measured, in contrary with the modeled monthly values. The modeled BC and OC fractions of $PM_{2.5}$ are usually underestimated with a few exceptions. In case of OC, a slightly better agreement is achieved for DJF. In JJA, however, the model is unable to reproduce values over $5\,\mu g\,m^{-3}$, often seen in measured data.

Over urban stations, the model is correlated very low with measurements and tends to underestimate the fine particulate matter concentrations in JJA, in contrary to the rural stations. In terms of other metrics, the model performs similarly than over rural stations.

4.2 Impact of city emissions on air quality

The impact of urban emissions from large cities on the regional air quality is evaluated in terms of selected air quality measures. For quantifying the exposure of the ecosystems, particularly crops, to elevated ozone levels, a widely used measure, the accumulated exposure over the threshold (AOT), introduced by Fuhrer et al. (1997), can be used. In this study, we evaluated the present AOT for the threshold of 40 ppbv for crops and forests (AOT40crop/forest) where the integration is done from May to July and from April to September, respectively. Further, the number of exceedances

Table 3. Comparison of model data with measurements: city-based evaluation of the correlation coefficient (r), root mean square error (RMSE; in $\mu g\,m^{-3}$), normalized mean square error (NMSE), the ratio of standard deviations (σ_r) and fractional bias (FB; in %) for hourly (for gases) and daily (for $PM_{2.5}$) averages for winter (DJF) and summer (JJA) months and for the whole year ("annual") for pollutants O_3, NO_2, SO_2 and $PM_{2.5}$.

		Ozone					NO_2					SO_2					$PM_{2.5}$				
		r	RMSE	NMSE	σ_r	FB	r	RMSE	NMSE	σ_r	FB	r	RMSE	NMSE	σ_r	FB	r	RMSE	NMSE	σ_r	FB
Vienna	Annual	0.55	35.04	0.64	1.17	−22	0.28	26.76	0.66	0.98	0	0.14	15.21	6.58	0.31	110	0.12	17.64	1.21	1.93	−49
	DJF	0.22	28.09	1.10	1.16	−31	0.30	25.05	0.54	1.34	13	0.03	22.12	5.98	0.35	116	0.18	26.26	1.91	3.07	−82
	JJA	0.38	37.53	0.34	1.24	9	0.19	28.14	0.95	0.79	8	0.07	3.78	1.89	0.62	52	−0.03	10.07	0.64	0.63	−2
Prague	Annual	0.57	33.89	0.73	1.19	−26	0.25	24.37	0.65	1.02	−21	0.26	20.12	4.32	0.34	111	0.04	19.97	1.81	1.73	−58
	DJF	0.23	26.31	1.32	1.05	−37	0.30	22.93	0.46	1.31	−6	0.14	29.47	4.11	0.40	116	0.28	27.36	2.79	4.26	−90
	JJA	0.48	35.49	0.35	1.26	12	0.13	24.55	1.07	0.85	−34	0.14	6.62	1.70	0.54	71	−0.04	14.76	1.13	0.47	−2
Frankfurt	Annual	0.70	28.22	0.31	1.25	−3	0.38	12.54	0.85	1.13	−29	0.23	10.42	2.97	0.41	66	0.05	23.51	2.58	2.21	−86
	DJF	0.44	21.59	0.46	1.00	−13	0.34	14.25	0.58	1.05	−12	0.14	16.09	3.17	0.48	89	0.28	34.03	4.52	5.54	−113
	JJA	0.60	29.79	0.18	1.45	4	0.12	10.51	1.37	1.37	−41	0.07	2.47	0.78	0.64	29	0.02	13.09	0.95	0.47	−19
Berlin	Annual	0.61	32.89	0.50	1.21	−12	0.33	17.30	0.93	0.86	−24	0.21	11.63	4.86	0.40	79	0.07	21.51	1.45	1.12	−45
	DJF	0.44	24.95	0.76	1.08	−32	0.34	17.74	0.62	1.03	−19	0.17	17.10	4.48	0.39	95	0.15	26.15	1.69	2.02	−71
	JJA	0.56	34.00	0.29	1.34	2	0.11	15.73	1.52	0.65	−34	0.06	3.79	2.62	0.93	10	0.12	14.15	1.54	0.74	−21
Munich	Annual	0.54	34.77	0.59	1.09	−20	0.20	32.94	1.09	1.25	−53	0.23	7.30	1.55	0.61	39	−0.03	16.41	1.07	0.91	−39
	DJF	0.32	29.70	1.00	0.89	−37	0.27	38.81	1.38	1.58	−76	0.24	8.73	1.10	0.64	21	0.46	19.72	1.17	2.37	−79
	JJA	0.50	36.98	0.33	1.09	16	0.16	27.51	0.94	0.98	−30	−0.04	4.71	0.94	0.45	23	−0.11	17.81	1.14	0.19	−26
Budapest	Annual	0.60	37.42	0.69	1.32	−6	0.22	30.26	1.09	1.47	−20	0.21	50.20	17.83	0.09	152	0.17	16.90	1.98	2.63	−72
	DJF	0.30	26.90	1.43	1.32	−19	0.22	31.00	0.89	1.93	−23	0.05	82.63	18.06	0.08	164	0.07	25.35	2.57	4.08	−99
	JJA	0.45	41.21	0.36	1.52	1	0.16	28.37	1.28	1.19	−14	−0.01	12.44	5.85	0.14	115	0.06	7.53	0.77	0.58	−11
Milan	Annual	0.62	41.15	1.09	1.21	−10	0.14	42.20	0.71	1.05	−6	0.45	41.17	5.76	0.26	132	0.15	38.93	2.08	3.10	−78
	DJF	0.17	22.68	2.38	0.58	−29	0.22	41.84	0.50	1.55	−25	0.21	59.04	3.73	0.27	121	0.03	63.83	2.86	3.92	−115
	JJA	0.39	51.86	0.51	1.28	9	0.22	47.44	1.52	0.64	−38	−0.08	16.38	4.91	0.34	130	0.05	11.96	0.62	0.61	−1
Katowice	Annual	0.62	34.30	0.85	1.22	−17	0.31	24.54	0.63	1.03	−8	0.31	69.92	3.65	0.37	105	−0.16	20.07	0.89	1.12	−25
	DJF	0.32	23.37	2.03	1.15	−42	0.34	25.85	0.49	1.12	−3	0.14	94.40	2.73	0.44	97	0.00	18.97	0.51	2.24	−13
	JJA	0.52	37.14	0.37	1.50	2	0.17	26.49	1.13	1.25	−24	0.09	28.17	2.95	0.39	100	−0.08	15.99	0.80	0.43	19
Warsaw	Annual	0.58	31.92	0.66	1.14	−11	0.28	23.79	0.76	1.14	−14	0.20	61.58	6.59	0.31	121	0.12	20.39	0.88	1.86	−43
	DJF	0.35	24.70	1.17	1.11	−44	0.27	20.64	0.47	1.09	−2	0.05	86.24	5.10	0.36	118	0.13	26.03	1.25	2.83	−45
	JJA	0.46	32.69	0.31	1.34	11	0.16	24.86	1.38	1.29	−36	0.04	22.29	4.86	0.35	105	−0.19	18.73	0.85	1.21	−57
Ljubljana	Annual	0.64	40.08	0.61	1.36	−33	0.36	21.94	0.94	1.44	−45	0.26	8.80	3.04	0.63	63	0.05	23.29	3.02	3.53	−104
	DJF	0.11	31.75	1.29	1.22	−51	0.25	27.41	0.88	1.53	−49	0.12	12.70	1.99	0.65	54	0.02	37.13	4.42	6.10	−130
	JJA	0.52	46.27	0.39	1.80	−31	0.21	17.14	1.05	1.30	−41	0.00	2.94	2.31	1.23	38	0.15	9.81	0.99	1.17	−68

Table 4. The EC air quality standards and AOT40 (in $\mu g\,m^{-3}$ and ppbv h, respectively) for different averaging interval. (+): the average concentration is evaluated instead of the number of the exceedances. (–): no threshold value defined.

Averaging interval	O_3	NO_2	SO_2	$PM_{2.5}$
Hourly	–	200	350	–
Daily	120 (8 h max)	–	125	–
Annual	–	+	+	+
DJF	–	–	+	+
JJA	+	–	–	–
AOT (crop/forest) JJA	+	–	–	–

above a certain threshold is evaluated for daily maximum 8 h running ozone mean, the hourly NO_2 and SO_2 and the daily SO_2 values. Finally, the mean JJA O_3, mean DJF and annual SO_2 and the mean annual $PM_{2.5}$ surface concentrations are considered. These measures are established in the EC Directive on ambient air quality and cleaner air for Europe (2008/50/EC) and are implemented also in the Czech legislation. These are summarized in Table 4.

Further in the paper, we will present the spatial distributions of the (1) absolute change of the chosen metrics by the introduction of city emissions (calculated as experiment 05BASE minus 05ZERO) and the (2) relative change which is calculated differently for ozone and for other pollutants. In the case of ozone, which (as we will see further in the paper) both increases and decreases, the change is shown relative to the no-urban emission case (05ZERO). For all other species, the change is shown relative to the all-emission case (05BASE), i.e. we are interested in the relative contribution. We also calculated the all-city-average of the maximum impact which coincides with the location of the cities themselves, summarized in Table 5.

4.2.1 Ozone

The impact of urban emissions on the average JJA surface ozone concentration (Fig. 6) is characterized by a clear reduction peaking over city centers from −4 ppbv over smaller cities up to −12 ppbv over western Germany urban agglomerations (e.g. Rhur area). This corresponds to a more than 30 % ozone decrease. Further inland or over the southern part of the domain, the influence of city emissions is smaller in relative sense with change around −20 % while the city influence peaks around −4 to −6 ppbv. Over rural regions, JJA ozone tends to decrease slightly for the western part of the domain. However, over the southern and eastern part of the domain, the mean JJA ozone concentrations increase due to city emissions by up to 0.5 ppbv, representing a 1 % increase. The average decrease over cities is −5.1(±3.3) ppbv, or −34.1(±18.3) %.

Table 5. The averaged maximal impact of urban emission on air quality (in terms of the quantities from Table 4) over cities. The 2nd and the 5th column stands for the absolute impact, the 3rd and the 6th column for the relative impact (for ozone related quantities) and contribution (for other species). The standard deviation of the all-city-average is included as well.

measure	absolute change	relative change (%)
O_3 JJA (ppbv)	−5.1(±3.3)	−34.1(±18.3)
AOT40crop (ppbv h)	−1800(±1300)	−29.1(±18.3)
AOT40forest (ppbv h)	−2460(±1800)	−30.7(±18)
O_3 over 120 $\mu g\,m^{-3}$	−2.9(±4.0)	−28.7(±39.8)
NO_2 annual ($\mu g\,m^{-3}$)	12.8(±6.8)	42.7(±18.3)
SO_2 annual ($\mu g\,m^{-3}$)	14.6(±16.7)	41.4(±24.4)
SO_2 winter ($\mu g\,m^{-3}$)	21.8(±26.0)	38.6(±23.8)
SO_2 over 125 $\mu g\,m^{-3}$	8.6(±18.9)	40.1(±44.8)
SO_2 over 350 $\mu g\,m^{-3}$	15.1(±43.0)	23.8(±40.0)
$PM_{2.5}$ ($\mu g\,m^{-3}$)	4.2(±3.7)	24.3(±12.8)

The impact on AOT40 values are, similar to the JJA average ozone, characterized by a significant decrease over and around cities up to −4000 ppbv h (for both impact on crops and forests) or −40 to −60 % in relative sense. An opposite impact is modeled over areas neighboring or even further from cities. City emissions increase AOT40 values up to 600 ppbv h over many regions, meaning an 5–10 %. In the vicinity of many cities (Milan, Zagreb, Warsaw), both AOT40s increase by up to 1000 ppbv h while the above-mentioned decrease occurs just a few 10 km towards the city center. The averaged decrease over cities is −1800(±1300) ppbv h or −29.1(±18.3) % for crops and −2460(±1800) or −30.7(±18) for forests, respectively.

A similar picture to previous ones is obtained when evaluating the number of days with maximum 8 h ozone greater than 120 $\mu g\,m^{-3}$. City emissions clearly decrease this number over and near cities (by up to −15 days yr^{-1}), but further from them, the increase of extreme ozone days is evident (up to 6 days yr^{-1}). This corresponds to 10 % increase over many parts of western Europe up to more than 40 % enhancement in central Europe with selected regions encountering even higher, up to a 100 % increase. The all-city-average decrease of the number of exceedances was calculated to −2.9(±4.0) or −28.7(±39.8) %.

4.2.2 Nitrogen oxides

Due to systematic negative bias the model was unable to predict exceedances over 200 $\mu g\,m^{-3}$, therefore only the impact of city emissions on the annual NO_2 concentration is shown (Fig. 7). The annual mean change can be as high as 30 $\mu g\,m^{-3}$ over the cities themselves, making around 50 % contribution to the absolute values over the western part of the domain, while over Central European cities (e.g. Berlin, Warsaw, Vienna, Budapest) it can reach 70 %. Over areas further from cities, the contribution quickly decreases making less

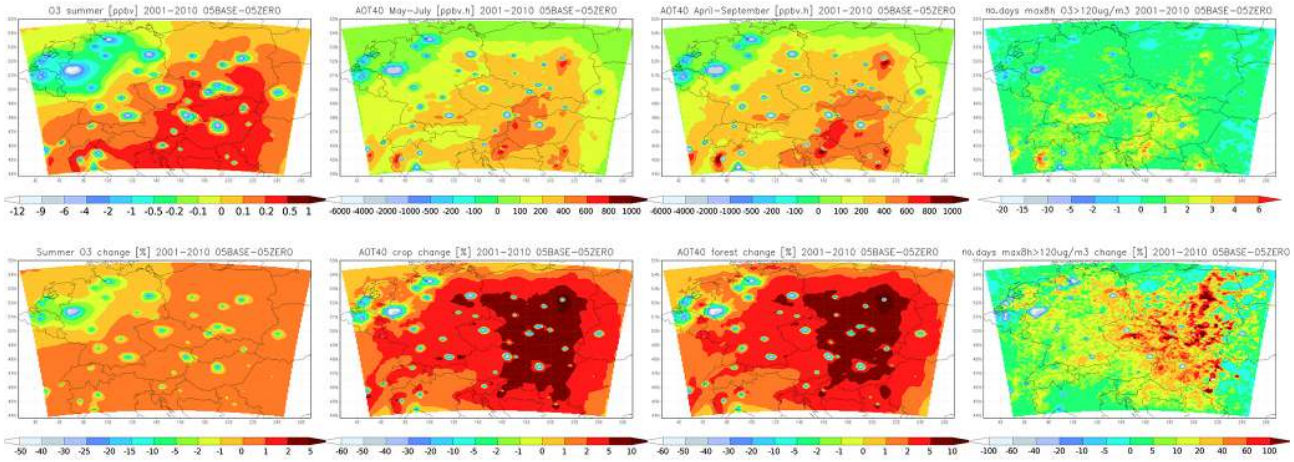

Figure 6. Impact of city emissions on ozone related air quality measures listed in Table 4. Upper row presents the absolute change averaged over 2001–2010. The lower row corresponds to the change relative to the zero urban emission case (05ZERO).

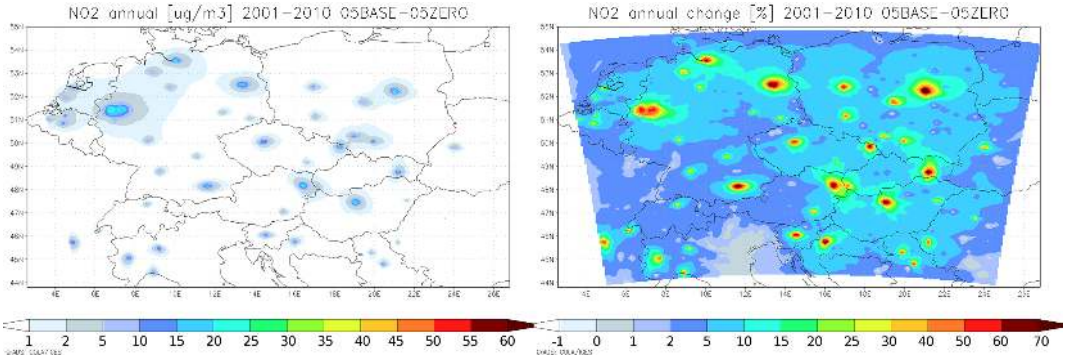

Figure 7. Impact of city emissions on the annual NO_2 concentration. Left figure presents the absolute change averaged over 2001–2010, while the relative contribution due to city emissions is shown on the right.

than 10 % of the absolute NO_2 values but remaining above 5 % over much of the domain. Comparing the absolute NO_2 change over cities and the JJA ozone decrease in previous figure it is clear that the larger the urban NO_2 perturbation, the more pronounced the ozone suppression. Indeed, linear fit between these two quantities (the plot not shown here) has a coefficient of determination $R^2 = 0.86$ indicating a strong link. The averaged urban induced NO_2 increase over cities is 12.8($\pm$6.8) $\mu g\,m^{-3}$, corresponding to 42.7($\pm$18.3) % contribution to the total value.

4.2.3 Sulfur dioxide

Figure 8 shows the impact on SO_2. The annual mean increase due to city emissions reaches 50 $\mu g\,m^{-3}$ over Eastern European cities and can be as high as 12 $\mu g\,m^{-3}$ over Western Europe (e.g. the Ruhr area). In relative manner, the contribution peaks at 80 % and is above 70 % over many cities all over the domain. However, it can stay higher even further from the cities: over large parts of northern Germany, the contribution to the annual SO_2 values is between 10 and 20 %. A similar picture is revealed when looking at the DJF SO_2 impact with up to 20 $\mu g\,m^{-3}$ increase over the cities themselves giving relative contribution of similar magnitude as in the case of the annual means (up to 80 % in cities). The all-city-average increases of annual and winter values are 5.5($\pm$6.3) and 8.2 ($\pm$9.8) $\mu g\,m^{-3}$, or 41.4($\pm$24.4) and 38.6($\pm$23.8) % as contributions, respectively.

The urban emissions contribution to the daily SO_2 exceedances over the 125 $\mu g\,m^{-3}$ threshold is again highest over cities making more than 20 days yr^{-1} contribution. Over Eastern Europe, larger regions are affected with city emissions increasing the number of exceedances by 1–2 days. In a relative sense, larger areas around cities are affected by higher daily SO_2 values often reaching 90–100 % meaning that the vast majority of the high SO_2 occurrences are due to emissions from cities. Even further from cities, especially over Eastern Europe, up to 10 % of all the elevated daily SO_2 values are due to city emissions. The impact on hourly SO_2 exceedances is again highest over cities (so in line with the emissions) with up to 100 h yr^{-1} contribution to the ab-

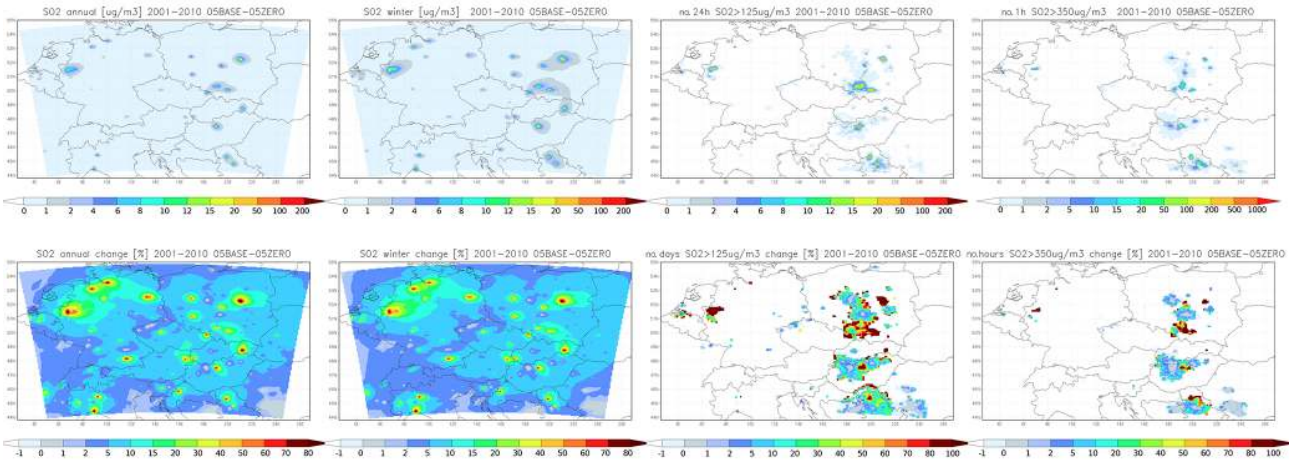

Figure 8. Impact of city emissions on SO_2 related air quality measures listed in Table 4: upper row shows the absolute change, the lower row the relative contribution from the urban emissions.

solute number of exceedances and, in general, Central and Eastern Europe is affected the most. Increases in hourly exceedances due to urban emissions are modeled at even larger distances from cities (similarly to daily exceedances) up to 1–2 h yr^{-1}. In relative numbers, the contribution is around 80–90 % over cities, but quickly reduces below 20 % further from them. The averaged increases in exceedances over cities are very variable: 8.6(±18.9) and 15.1(±43.0) for the daily and hourly averaging period, giving 40.1(±44.8) % and 23.8(±40.0) % relative contribution.

4.2.4 $PM_{2.5}$

According to Fig. 9, urban emissions increase annual $PM_{2.5}$ levels by 4–8 µg m^{-3} over cities with the highest impact over the Ruhr area and Warsaw (up to 15 µg m^{-3}). These correspond to about 20–60 % contribution to the total $PM_{2.5}$ levels. Above rural areas further from cities, the impact goes rapidly below 1 µg m^{-3}. However, in a relative manner, it remains around 5–10 %, e.g. over Northern Germany or Central Europe. The averaged urban induced $PM_{2.5}$ increase over cities is 4.2(±3.7) µg m^{-3}, corresponding to 24.3(±12.8) % contribution to the total value.

4.2.5 Impact on a particular city

It was seen in Figs. 6–9 that urban emissions impact air quality mainly over the cities themselves and the influence on rural air is much smaller. The question is how the emissions from other cities contribute to the impact over a particular city, or in other words, what fraction of the total impact (due to all cities) is attributable to the impact of the local emissions. To examine this, we selected the city of Prague lying in the center of the domain and representing a middle-sized city from the domain. Figure 10 presents the total impact (i.e. from all urban emissions; left column) and the impact of emissions from the rest of the cities not considering the emissions from Prague (right column). We evaluated this in terms of the average quantities from Table 4 (annual, DJF and JJA means), showing only the relevant part of the domain. The total impact (right column) actually corresponds to a detail of the impact presented in Figs. 6–9. and gives −7 ppbv, 15, 6, 8, 3 µg m^{-3} as the maximum change over Prague due to all urban emissions for JJA O_3, annual NO_2, annual and DJF SO_2 and annual $PM_{2.5}$. The same quantities from the right column give, for Prague, approximately 0.2 ppbv, 0.5, 0.4, 0.6, 0.5 µg m^{-3}. This represents about 3, 3, 7, 7, 16 % of the impact due to all urban emissions.

4.2.6 Sensitivity experiments

The response to possible urban emission reductions of selected ozone related measures presented in Table 4 is evaluated here. The results are presented in Fig. 11. Reducing city NO_x emissions by 20 %, due to limited reaction with NO, JJA ozone concentrations are enhanced by around 1.5–2 ppbv over city centers but O_3 increases over larger areas as well, although by a much smaller magnitude (0.1–0.2 ppbv increase over Western Germany). The AOT40s responded in a similar manner: due to reduced ozone titration, elevated AOT40s are modeled over and around cities (by up to 500–1500 ppbv h). However, over Central and Southern Europe, AOT40s tend to slightly decrease (by up to −200 ppbv h) with decreasing urban NO_x emissions. The reduced titration is evident on the change in the number of ozone exceedances which increases over cities often by more than 2–3 days yr^{-1}. Further from urban centers, however, less NO_x emitted tend to decrease ozone exceedances (especially over Central Europe, by up to −1.5 days yr^{-1} in average).

While NO_x reduction increased ozone over cities, and caused small decreases elsewhere, especially in terms of occurrences of higher values, reduced NMVOC emissions

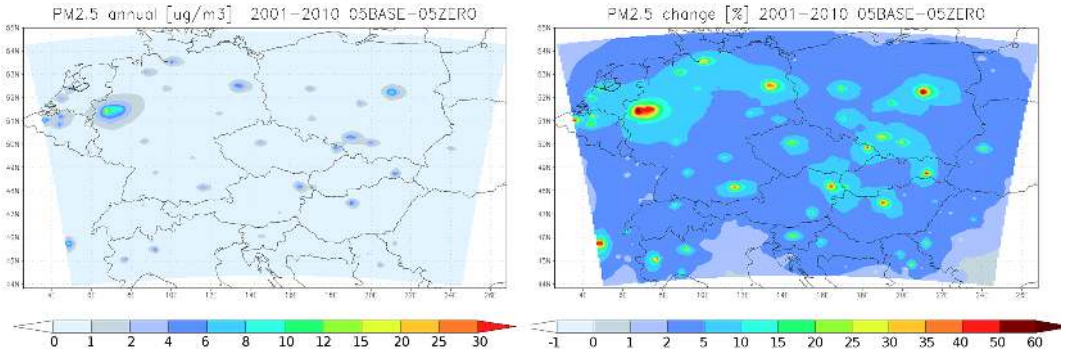

Figure 9. Impact of city emissions on the annual $PM_{2.5}$ concentration. Left figure presents the absolute change averaged over 2001–2010, while the relative contribution due to city emissions is shown on the right.

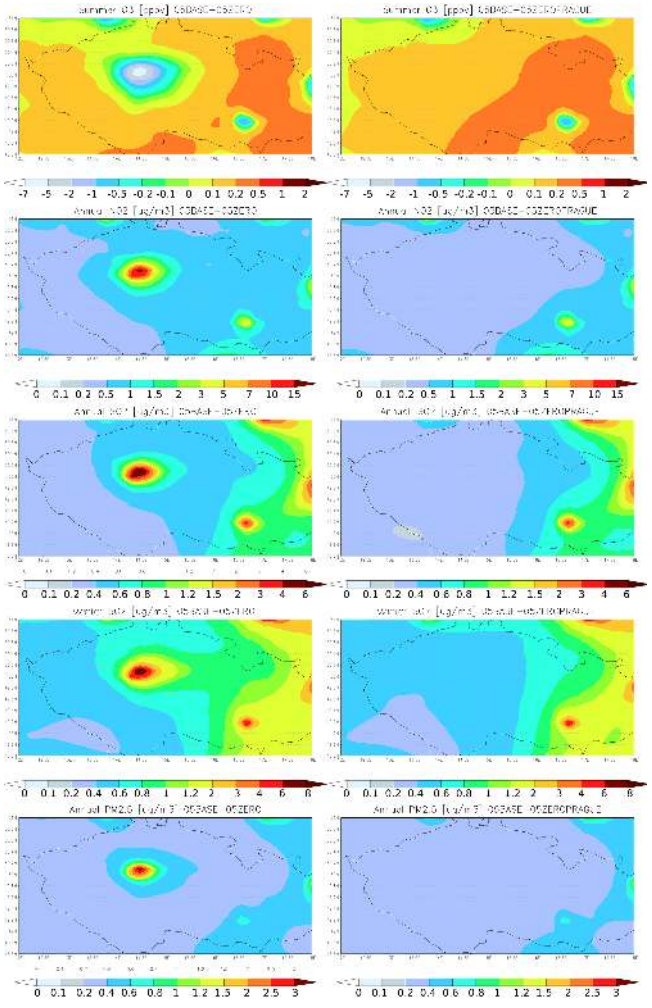

Figure 10. Impact of city emissions on average O_3 (ppbv; summer), NO_2 ($\mu g\,m^{-3}$; annual), SO_2 ($\mu g\,m^{-3}$; annual and DJF) and $PM_{2.5}$ ($\mu g\,m^{-3}$; annual). Left column: impact of all cities, right column: impact off all cities except Prague.

cause ozone decrease all over the domain. In terms of JJA average O_3, it is highest over cities, up to -0.3 ppbv. Decreases are modeled for AOT40s (up to -400 ppbv h) and for the number of exceedances (up to -1–2 days yr^{-1}) as well.

The simultaneous reduction of both NO_x and NMVOC leads to similar changes in JJA ozone means values: only the peak changes over cities – caused by decreased titration, are smaller, up to 1.5 ppbv. In terms of AOT40crop/forest, reduction of urban NO_x + NMVOC emissions leads to increases over cities, but again by a smaller magnitude than in case of purely NO_x reduction. On the other hand, over rural areas, AOT40s decreased more than due to NO_x reduction alone. The increases of 8 h ozone exceedances due to decreased NO_x + NMVOC go up to 2–3 days yr^{-1}, which is again less than for NO_x reduction. On the other hand, again, the decrease in the number of exceedances over rural areas is slightly larger in case of simultaneous NO_x + NMVOC reduction than due to NO_x emission reduction only.

5 Discussion

The validation of the modeling system

The validation showed that the modeling system captures the observed annual cycle of ozone with negative bias encountered in each month except late summer and autumn. The chemical boundary conditions used by our model were taken from a 10-year simulation from a larger domain, which however was forced with time invariant, spatially constant boundary conditions (40 ppbv) and this artificial constraint could propagate to the inner domain. Katragkou et al. (2010) showed that the final ozone levels greatly depend on the imposed boundary conditions. This constant constrain is also evident in the underestimation of the standard deviation for each averaging period, especially for DJF. The diurnal cycle underlines the monthly model bias, giving lower hourly values in DJF and better agreement in JJA, but with an underestimation of the JJA daily maximum values. The lower afternoon values of ozone in JJA can be attributed also by

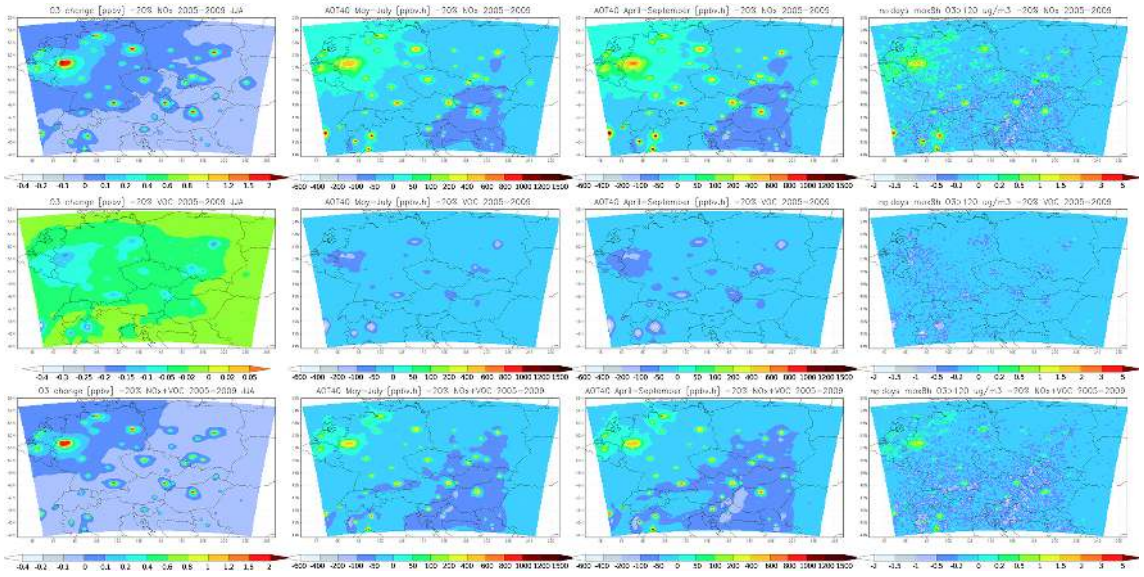

Figure 11. Impact of 20 % reduction of NO_x (upper row), 20 % reduction of NMVOC (middle row) and 20 % reduction of both NO_x and NMVOC (bottom row) on ozone related air quality measures: average JJA ozone, AOT40 for crops and forest, and, the average number of days with maximum 8 h ozone running mean greater than 120 $\mu g\,m^{-3}$.

higher afternoon and evening NO_2 values, as a result of the $NO + O_3$ reaction. A very similar result is provided by Huszar et al. (2012) both in terms of monthly and hourly variation.

Recently, Akritidis et al. (2013) were investigating the impact of CBC on the simulated ozone concentrations using the same two models as in our study (an offline couple of models RegCM and CAMx). They found a clear improvement in the correlation coefficient when using global chemistry model (ECHAM5/MOZART) based CBC. Their correlation of monthly ozone values using time/space invariant CBCs is 0.74 that compares very well to our value (0.77). Introducing the MOZART based CBCs, the correlations often increased by more than 0.1.

Compared to Huszar et al. (2012), our modeling system performs better in terms of correlation, with $r = 0.6$ and $r = 0.67$ for hourly and daily values against 0.51 and 0.53 in the later study which used an earlier version of the RegCM-CAMx coupled system. This improvement probably lies in the duration of the data of comparison: in a 10-year time frame, the main drivers of the variability are the diurnal and monthly variations which contribute to an overall correlation in a significant way (Hogrefe et al., 2001). Zanis et al. (2011), who used the same models in offline couple for also a 10-year experiment over Europe, achieved similar values of correlations. In general, our model performs for ozone better during JJA, when photochemistry is more intensive. This is true also for RMSE, NMSE and FB. Katragkou et al. (2010) and Zanis et al. (2011) came to the same conclusion.

Very low correlations are achieved in case of NO_2, especially for the hourly values. In general, it is difficult to achieve a higher degree of agreement in case of precursor species for at least two reasons. The driving meteorology, which greatly influences the hour-to-hour evolution of the NO_2 concentrations, is a result of a 10-year climate model run. The climate model does not need to accurately reproduce the hour-to-hour, day-to-day weather pattern; however it has to reconstruct the climate close to reality in terms of averaged quantities and capability to capture extremes (Halenka et al., 2006). Further, the emission decomposition into hourly values is based on numerous assumptions about the typical temporal evolution of a certain activity sector and the actual emissions may differ for a particular hour. At last, ozone precursor species are modeled always with a higher degree of uncertainty with great differences between models and setups (including chemistry mechanism) while they give very similar results in terms of final ozone concentrations (Kuhn et al., 1998).

Another striking feature is the underestimation of the modeled NO_2 values. Huszar et al. (2012), who encountered a similar negative model bias, concluded that one reason lies in the overall underestimation of emissions and in the suppressed NO to NO_2 conversion due to volatile organic compounds in CB-IV mechanism. Our configuration invoked the CB-V chemistry mechanism which was to remove this erroneous feature in the earlier version of the CB mechanism (Sarwar et al., 2008). However, the negative bias persists in our simulations, which in consequence could mean that the emissions are probably underestimated for the region modeled. Further, seen in the hourly plots, the underestimation mainly occurs during night-time similarly as in Huszar et al. (2012). Many other studies argued that chemistry in

air quality models performs less biased during daylight (Zanis et al., 2011). At last, biomass burning emissions were not accounted for in our simulations while it is an important contributor to NO_2 burdens, especially for southern stations (Baldasano et al., 2011).

The strong DJF overestimation of the SO_2 levels in Huszar et al. (2012) was attributed to inadequate treatment of emissions in considering them as only area sources. An important improvement in the RegCMCAMx4 model against its earlier version was the treatment of part of SO_2 emissions as elevated source which better compiles with the reality. However, our results suggest a minor improvement in DJF and the positive bias, although smaller, remained. On the other hand, summer encounters a clear negative bias. This could indicate that both the incorrect monthly disaggregation of the annual SO_2 emissions and the overestimated conversion to sulfate aerosol (in JJA) play a role here as well. Reduced deposition can contribute to SO_2 overestimation (Baker and Scheff, 2007) as well, as concluded by Huszar et al. (2012) who applied the same deposition scheme as in this study.

To understand the model performance concerning the $PM_{2.5}$ levels, we have to look at the comparison of the main fine particle matter components. In DJF, $PM_{2.5}$ is largely underestimated: the main contributors to this bias is the underestimation of nitrate aerosol and both black and organic carbon. The DJF sulfate aerosol is in acceptable agreement with the observations, which, given that SO_2 is overestimated, means that the SO_2 to SO_4 conversion is underestimated, leading to fair observation-model agreement. During JJA on the other hand, probably too strong SO_2 to SO_4 transition occurs, resulting in (1) SO_2 concentrations even more negatively biased and (2) an overestimated sulfate aerosol. Huszar et al. (2012) achieved better agreement for PSO_4 than for SO_2 arguing that, again, precursor species are often simulated with lower accuracy than secondarily formed pollutants. Baker and Scheff (2007), who used CAMx with the same chemistry mechanism and aerosol module (ISORROPIA) arrived at the same conclusion. This is however not true for nitrate aerosol in our experiments, which shows a reasonable agreement (at least in terms of range of simulated values) with observations for JJA, but DJF model values are greatly underestimated. Bessagnet et al. (2004) encountered the opposite situation, they had larger difficulties to capture JJA values than those during DJF. In our case, the DJF underestimation is probably connected with less NO_2 simulated during this season. Similar underestimation occurs in the study of Myhre et al. (2006), especially for high concentrations. In general, the secondary inorganic aerosol model biases can be attributed to overall difficulties in simulating heterogeneous and aqueous phase processes (Bessagnet et al., 2004).

Black carbon is usually underestimated in both DJF and JJA, in a similar extent than in Huszar et al. (2012). Schaap et al. (2004) obtained comparable values as well and attributed this negative model bias to deficiencies in describing coating processes which are burdened by large uncertainties and directly determine the BC lifetime (BC has to become hydrophilic to get washed out by the wet deposition). Even more striking underestimation occurs for the organic carbon, although this bias is reduced compared to Huszar et al. (2012). This is probably due to different emission data used here for primary OC. However, the largest source for low modeled OC values probably lies in (1) in modeling the gas-to-particle partitioning that is affected with uncertainty with a large number of tunable parameters (Simpson et al., 2007), (2) disregarding biomass burning aerosol that occurred in 2003 in eastern Europe affecting the measurements of Yttri et al. (2007).

As expected, for selected urban stations, our modeling system is, in general, less accurate, especially in terms of correlations. Urban stations are often influenced by local or nearby emissions sources, far below the models spatial resolution. The relatively coarse input emissions data cannot resolve the variability of these sources leading to much worse observation-model agreement compared to rural background stations. In case of ozone, the model over urban stations is positively biased in summer, which can be explained by the instant dilution of concentrated urban emission into the 10 km model grid which tends to overestimate ozone production (Hodnebrog et al., 2011). The opposite holds for the modeled NO_2 concentrations which, due to instant dilution, are negatively biased in the model within urban environment. The model performance for SO_2 and $PM_{2.5}$ is worse as well over urban stations compared to rural ones, probably for the same reasons as for ozone and NO_2.

The urban emissions impact on air quality

Generally, the impact of city emissions on ozone is characterized by two main features: over cities, all examined metrics decreased. Enhancements are encountered further from urban centers and are of lower magnitude than the decreases. Im et al. (2011a, b) performed regional chemistry simulations over Istanbul and Athens and arrived at similar results: decrease of O_3 over urban areas due to reaction with NO and, as a consequence of NMVOC transport, a smaller production of O_3 at downwind areas due to increasing NMVOC / NO_x ratio. Previously, Poupkou et al. (2008) showed that regional transport plays and important role in carrying urban pollution to larger distances leading to O_3 formation downwind from cities. Im and Kanakidou (2012) focused on both Istanbul and Athens and found up to 27 and 5 ppbv decreases of ozone due to urban emissions from these cities. Although they are not covered by our domain and are characterized by warmer climate, the changes are consistent with our JJA mean changes, especially in the case of Athens, which is affected by higher background pollution (Kanakidou et al., 2011) as is typical for cities over our domain as well.

Our results further suggest that while the enhancement of average ozone further from cities (as a result of downwind

transport) is relatively small (up to 0.5 ppbv), however, a much larger increase is detected when considering metrics describing accumulated and extreme ozone values. In conclusion, the importance of cities' impact on ozone levels lies in higher potential for extreme ozone pollution over downwind areas during favorable meteorological conditions rather than in an increase of average levels. This is seen especially in changes in the number of exceedances, but the AOT40 levels show often large enhancements around cities as well.

The impact on NO_2 levels is important only over cities themselves indicating that in urban plume further from urban areas, the NO_x ages to HNO_3 decreasing the contribution to the total NO_2 levels. The contribution in cities goes up to 50–70 % indicating that a large part (i.e. 30–50 %) of the urban NO_2 pollution is of non-urban origin. This supports region- or country-wide emission control strategies as their emissions undergo regional transport. Im and Kanakidou (2012) found for Athens and Istanbul an even larger contribution around 95–96 % over these cities. Earlier, Guttikunda et al. (2005) calculated the eastern Asia megacities contribution to NO_z levels and found values around 10–30 % over cities, however NO_z contains species produced during plume aging further from city centers causing this lower contribution.

In terms of average quantities (annual and DJF mean), the urban sulfur dioxide contribution is similar to NO_2 contribution. Urban SO_2 emissions are responsible for up to 70–80 % of pollution over urban areas themselves. In other words, 20–30 % of urban SO_2 pollution comes from other areas (rural and minor cities, villages) giving importance to the regional emission transport. Guttikunda et al. (2003) found over 50–75 % contribution near megacities of eastern Asia and 10–30 % over large areas in eastern China far from megacities. Similar values are obtained in our simulations (around 10–20 %) over large parts of the domain. They argue that large contribution within the cities indicate that the industry is concentrated within urban areas. This is often the case for eastern European cities where we obtained the highest urban SO_2 contributions. The urban contribution to SO_2 daily and (mainly) hourly exceedances is slightly higher than the contribution to average values and much more resembles the emission pattern indicating the enhanced importance of local urban emission in high air pollution episodes (when these exceedances occur) compared to the inter-urban pollution transport.

The annual average $PM_{2.5}$ impact calculated in our simulations (up to 10–15 $\mu g\,m^{-3}$) is in line with values obtained for Istanbul and Athens from Im and Kanakidou (2012): 18 and 12 $\mu g\,m^{-3}$, respectively. However, their relative contribution is higher due to probably lower background pollution (around 62 and 55 %, respectively) compared to ours (30–60 % contribution over cities).

The emission reduction sensitivity test showed that in cities, the chemical regime is NO_x-saturated meaning it is dominated by the reaction of NO with O_3. This causes that NO_x-oriented emission reduction to actually worsen the ozone levels above cities and its close environment. This holds for the AOT40s and exceedance change as well, where decreases are modeled only far from cities, where the urban plumes undergo photochemical aging. The response to 20 % NMVOC emission reduction is less dominant and in terms of all metrics it leads to reduction of ozone. Im et al. (2011b) tested the ozone response to 30 % reduced NO_x or NMVOC emissions and found the ozone concentrations more sensitive to NO_x emissions than to VOC emission. They also showed that above and around cities, reduced (increased) NO_x emissions led to enhanced (suppressed) ozone by up to 8–10 % (in both direction), which is similar to the percentage change extracted from our simulations giving about 5–8 % ozone increase due to 20 % NO_x emission reduction. The smaller numbers can be partly due to the lower emission reduction scenario. In case of NMVOC emission reduction, our numbers (up to −2 %) are only half of the relative ozone reduction achieved in their study (up to −4 %). The small ozone decreases due to NO_x reduction in terms of AOT40s and exceedances further from cities in our simulations are probably caused by less NO_x available in urban plumes when it mixes with biogenic NMVOC emissions over downwind areas (Im et al., 2011a, b; Finardi et al., 2014).

Interestingly, the simultaneous NO_x + NMVOC reduction scenario led to a very similar ozone response than the NO_x reduction alone. This can be explained by the dominating effect of ozone titration due to NO_x emissions. Indeed, the NMVOC reduction caused only minor ozone changes. Consequently, the effective ozone reduction strategy depended on the targeted area. Urban emission reduction of NO_x and NMVOC improves the air-pollution over rural areas, however over the cities themselves, this usually leads to worsening of the ozone levels. According to our simulations, the only effective emission reduction strategy to decrease ozone levels is to reduce NMVOC emissions significantly while changing the NO_x emissions only slightly or not at all.

Compared to the impact of all (100 %) emissions, the 20 % NO_x + VOC emission change approximately equals to the 1/5th of the total impact (mainly for JJA ozone and AOT40s). This justifies the 100 % emission perturbation approach instead of a smaller perturbation introduced to maintain linearity. A similar approach was used recently for aviation emission impact (Huszar et al., 2013).

6 Conclusions

Answering the questions raised in the introduction, the air quality over cities is largely determined by the urban emissions but a considerable (often a few tens of %) fraction of the surface concentration is attributable to other sources from rural areas, minor cities (which we did not consider here) or transported from distant areas (via the boundary conditions). On the other hand, the contribution of urban emission to sur-

face pollution over rural areas is in general lower, around 5–10 %. It is further a question, how one city impacts the air pollution of other cities or, in other words, how is the air pollution in a certain city impacted by other cities. Huszar et al. (2014), who examined the urban land-surface forcing on regional climate (mainly temperature) using very similar modeling framework on the same domain as here, show that the urban impact on temperature is localized, meaning that there is only a minor influence of neighboring cities on a certain city (Prague, in their case). Here, for the impact of emissions on chemistry, it is shown for the case of Prague that the impact from "all-except-Prague" urban emissions on Prague is rather small (a few %, to over 10 % in case of $PM_{2.5}$) meaning that the air pollution over Prague is determined mainly by local urban sources rather than urban emissions from other cities. The inter-urban influence is largest for fine aerosol which has, in general, a longer lifetime giving more importance to long-range transport.

In summary, we showed that air pollution over urban areas is a combination of the local urban emissions and those from rural areas without large cities with this later having often more than 50 % contribution. This implies that to meet the air quality standards over cities, emission from the surrounding rural areas and long-range transport have to be considered as well. Further it is shown that the inter urban air-pollution is minor meaning that emissions from large cities do not influence each other in a significant way, at least as a long-term average.

It has to be emphasized that the long-term impact was evaluated here. Depending on the meteorological conditions (wind direction, temperature, boundary layer state), the impact of urban emissions represented by the urban-plume can be much larger than shown here, corresponding to the averaged impact.

Finally, numerous caveats of the modeling system were identified that have to be taken into account in future developments. The most important ones are inclusion of time/space variant chemical boundary conditions that highly affected ozone performance, improvement in the representation of the annual cycle of emissions, considering biomass burning emissions, inclusion of dust emissions and their radiative effects as well as those of secondary organic aerosol.

Acknowledgements. This work has been funded by the Czech Science Foundation (GACR) project No. 13-19733P and by the project UNCE 204020/2013. We further acknowledge the TNO MEGAPOLI emissions data set from the EU-FP7 project MEGAPOLI. (http://megapoli.info).

Edited by: K. Tsigaridis

References

Akritidis, D., Zanis, P., Katragkou, E., Schultz, M., Tegoulias, I., Poupkou, A., Markakis, K., Pytharoulis, I., and Karacostas, T.: Evaluating the impact of chemical boundary conditions on near surface ozone in regional climate–air quality simulations over Europe, Atmos. Res., 134, 116–130, doi:10.1016/j.atmosres.2013.07.021, 2013.

Baker, K. and Scheff, P.: Photochemical model performance for $PM_{2.5}$ sulfate, nitrate, ammonium, and precursor species SO_2, HNO_3, and NH_3 at background monitor locations in the central and eastern United States, Atmos. Environ., 41, 6185–6195, 2007.

Baklanov, A.: Chemical weather forecasting: a new concept of integrated modelling, Adv. Sci. Res., 4, 23–27, doi:10.5194/asr-4-23-2010, 2010.

Baklanov, A., Lawrence, M., Pandis, S., Mahura, A., Finardi, S., Moussiopoulos, N., Beekmann, M., Laj, P., Gomes, L., Jaffrezo, J.-L., Borbon, A., Coll, I., Gros, V., Sciare, J., Kukkonen, J., Galmarini, S., Giorgi, F., Grimmond, S., Esau, I., Stohl, A., Denby, B., Wagner, T., Butler, T., Baltensperger, U., Builtjes, P., van den Hout, D., van der Gon, H. D., Collins, B., Schluenzen, H., Kulmala, M., Zilitinkevich, S., Sokhi, R., Friedrich, R., Theloke, J., Kummer, U., Jalkinen, L., Halenka, T., Wiedensholer, A., Pyle, J., and Rossow, W. B.: MEGAPOLI: concept of multi-scale modelling of megacity impact on air quality and climate, Adv. Sci. Res., 4, 115–120, doi:10.5194/asr-4-115-2010, 2010.

Baldasano, J. M., Pay, M. T., Jorba, O., Gasso, S., and Jimenez-Guerrero, P.: An annual assessment of air quality with the CALIOPE modeling system over Spain, Sci. Total Environ., 409, 2163–2178, doi:10.1016/j.scitotenv.2011.01.041, 2011.

Barth, M. C. and Church, A. T.: Regional and global distributions and lifetimes of sulfate aerosols from Mexico City and southeast China, J. Geophys. Res., 104, 30231–30239, 1999.

Beekmann, M. and Derognat, C.: Monte Carlo uncertainty analysis of a regional-scale transport chemistry model constrained by measurements from the Atmospheric Pollution Over the Paris Area (ESQUIF) campaign, J. Geophys. Res., 108, 8559, doi:10.1029/2003JD003391, 2003.

Beekmann, M. and Vautard, R.: A modelling study of photochemical regimes over Europe: robustness and variability, Atmos. Chem. Phys., 10, 10067–10084, doi:10.5194/acp-10-10067-2010, 2010.

Behera, N. S. and Sharma, M.: Investigating the potential role of ammonia in ion chemistry of fine particulate matter formation for an urban environment, Sci. Total Environ., 408, 3569–3575, 2010.

Bessagnet, B., Hodzic, A., Vautard, R., Beekmann, M., Cheinet, S., Honoré, C., Liousse, C., and Rouil, L.: Aerosol modeling with CHIMERE–preliminary evaluation at the continental scale, Atmos. Environ., 38, 2803–2817, doi:10.1016/j.atmosenv.2004.02.034, 2004.

Borrego, C., Monteiro, A., Ferreira, J., Miranda, A. I., Costa, A. M., Carvalho, A. C., and Lopes, M.: Procedures for estimation of modelling uncertainty in air quality assessment, Environ. Int., 34, 613–620, doi:10.1016/j.envint.2007.12.005, 2008.

Butler, T. M. and Lawrence, M. G.: The influence of megacities on global atmospheric chemistry: a modelling study, Environ. Chem., 6, 219–225, doi:10.1071/EN08110, 2009.

Byun, D. W.: Dynamically consistent formulations in meteorological and air quality models for multiscale atmospheric studies. Part I: Governing equations in a generalized coordinate system, J. Atmos. Sci., 56, 3789–3807, 1999.

Chen, S. J., Liao, S. H., Jian, W. J., and Lin, C. C.: Particle size distribution of aerosol carbons in ambient air, Environ. Int., 23, 475–488, 1997.

Denier van der Gon, H. A. C., Kuenen, J., and Butle, T.: A Base Year (2005) MEGAPOLI Global Gridded Emission Inventory (1st Version), Deliverable D1.1, MEGAPOLI Scientific Report 10-13, MEGAPOLI-16-REP-2010-06, TNO Built Environment and Geosciences, Utrecht, the Netherlands, 2010.

Dickinson, R. E., Henderson-Sellers, A., and Kennedy, P.: Biosphere–atmosphere transfer scheme (BATS) version 1 as coupled to the NCAR community climate model, Tech Rep, National Center for Atmospheric Research Tech Note NCAR.TN387 + STR, NCAR, Boulder, CO, 1993.

Eben, K., Jurus, P., Resler, J., Belda, M., Pelikán, E., Krüger, B. C., and Keder, J.: An ensemble Kalman filter for short-term forecasting of tropospheric ozone concentrations, Q. J. Roy. Meteorol. Soc., 131, 3313–3322, doi:10.1256/qj.05.110, 2005.

EEA: Corine Land Cover 2006 technical guidelines, EEA (European Environment Agency), OPOCE (Office for Official Publications of the European Communities), Copenhagen, 2012.

Escudero, M., Lozano, A., Hierro, J., del Valle, J., and Mantilla, E.: Urban influence on increasing ozone concentrations in a haracteristic Mediterranean agglomeration, Atmos. Environ., 99, 322–332, doi:10.1016/j.atmosenv.2014.09.061, 2014.

Finardi, S., Silibello, C., D'Allura, A., and Radice, P.: Analysis of pollutants exchange between the Po Valley and the surrounding European region, Urban Climate, 10, 682–702, doi:10.1016/j.uclim.2014.02.002, 2014.

Folberth, G. A., Rumbold, S., Collins, W. J., and Butler, T.: Determination of Radiative Forcing from Megacity Emissions on the Global Scale, MEGAPOLI Project Scientific Report 10e08, UK MetOffice Hadley Center, Exeter, UK, 2010.

Freney, E. J., Sellegri, K., Canonaco, F., Colomb, A., Borbon, A., Michoud, V., Doussin, J.-F., Crumeyrolle, S., Amarouche, N., Pichon, J.-M., Bourianne, T., Gomes, L., Prevot, A. S. H., Beekmann, M., and Schwarzenböeck, A.: Characterizing the impact of urban emissions on regional aerosol particles: airborne measurements during the MEGAPOLI experiment, Atmos. Chem. Phys., 14, 1397–1412, doi:10.5194/acp-14-1397-2014, 2014.

Fritsch, J. M. and Chappell, C. F.: Numerical prediction of convectively driven mesoscale pressure systems, Part I: Convective parameterization, J. Atmos. Sci., 37, 1722–1733, 1980.

Fuhrer, J., Skärby, L., and Ashmore, M. R.: Critical levels for ozone effects on vegetation in Europe, Environ. Pollut., 97, 91–106, 1997.

Gaffney, J. S., Marley, N. A., Cunningham, M. M., and Doskey, P. C.: Measurements of peroxyacyl nitrates (PANS) in Mexico City: implications for megacity air quality impacts on regional scales, Atmos. Environ., 33, 5003–5012, 1999.

Giorgi, F., Bi, X., and Qian, Y.: Indirect versus direct effects of anthropogenic sulfate on the climate of east Asia as simulated with a regional coupled climate-chemistry/aerosol model, Climatic Change, 58, 345–376, 2003.

Giorgi, F., Coppola, E., Solmon, F., Mariotti, L., Sylla, M., Bi, X., Elguindi, N., Diro, G. T., Nair, V., Giuliani, G., Cozzini, S., Guettler, I., O'Brien, T. A., Tawfi, A. B., Shalaby, A., Zakey, A., Steiner, A., Stordal, F., Sloan, L., and Brankovic, C.: RegCM4: model description and preliminary tests over multiple CORDEX domains, Clim. Res., 52, 7–29, 2012.

Grell, G.: Prognostic evaluation of assumptions used by cumulus parameterizations, Mon. Weather Rev., 121, 764–787, 1993.

Grell, G. and Baklanov, A.: Integrated modeling for forecasting weather and air quality: a call for fully coupled approaches, Atmos. Environ., 45, 6845–6851, 2011.

Grell, G., Dudhia, J., and Stauffer, D. R.: A description of the fifth generation Penn State/NCAR Mesoscale Model (MM5), National Center for Atmospheric Research Tech Note NCAR/TN-398 + STR, NCAR, Boulder, CO, 1994.

Guenther, A. B., Zimmermann, P. C., Harley, R., Monson, R. K., and Fall, R.: Isoprene and monoterpene emission rate variability: model evaluations and sensitivity analyses, J. Geophys. Res., 98, 12609–12617, 1993.

Gurjar, B. R., Jain, A., Sharma, A., Agarwal, A., Gupta, P., Nagpure, A. S., and Lelieveld, J.: Human health risks in megacities due to air pollution, Atmos. Environ., 44, 4606–4613, doi:10.1016/j.atmosenv.2010.08.011, 2010.

Guttikunda, K. S., Carmichael, G. R., Calori, G., Eck, C., and Woo, J.-H.: The contribution of megacities to regional sulfur pollution in Asia, Atmos. Environ., 37, 11–22, doi:10.1016/S1352-2310(02)00821-X, 2003.

Guttikunda, S. K., Tang, Y., Carmichael, G. R., Kurata, G., Pan, L., Streets, D. G., Woo, J.-H., Thongboonchoo, N., and Fried, A.: Impacts of Asian megacity emissions on regional air quality during spring 2001, J. Geophys. Res., 110, D20301, doi:10.1029/2004JD004921, 2005.

Halenka, T., Kalvova, J., Chladova, Z., Demeterova, A., Zemankova, K., and Belda, M.: On the capability of RegCM to capture extremes in long term regional climate simulation – comparison with the observations for Czech Republic, Theor. Appl. Climatol., 86, 125–145, doi:10.1007/S00704-005-0205-5, 2006.

Haylock, M., Hofstra, N., Tank, A. K., Klok, E., Jones, P., and New, M.: A European daily high–resolution gridded data set of surface temperature and precipitation for 1950–2006, J. Geophys. Res., 113, D20119, doi:10.1029/2008JD010201, 2008.

Hodnebrog, Õ., Stordal, F., and Berntsen, T. K.: Does the resolution of megacity emissions impact large scale ozone?, Atmos. Environ., 45, 6852–6862, 2011.

Hodzic, A., Jimenez, J. L., Madronich, S., Canagaratna, M. R., DeCarlo, P. F., Kleinman, L., and Fast, J.: Modeling organic aerosols in a megacity: potential contribution of semi-volatile and intermediate volatility primary organic compounds to secondary organic aerosol formation, Atmos. Chem. Phys., 10, 5491–5514, doi:10.5194/acp-10-5491-2010, 2010.

Hogrefe, C., Rao, S. T., Kasibhatla, P., Hao, W., Sistla, G., Mathur, R., and McHenry, J.: Evaluating the performance of regional-scale photochemical modeling systems: Part II – ozone predictions, Atmos. Environ., 35, 4175–4188, doi:10.1016/S1352-2310(01)00183-2, 2001.

Huszar, P., Miksovsky, J., Pisoft, P., Belda, M., and Halenka, T.: Interactive coupling of a regional climate model and a chemistry transport model: evaluation and preliminary results on ozone and aerosol feedback, Clim. Res., 51, 59–88, doi:10.3354/cr01054, 2012.

Huszar, P., Teyssèdre, H., Michou, M., Voldoire, A., Olivié, D. J. L., Saint-Martin, D., Cariolle, D., Senesi, S., Salas Y Melia, D., Alias, A., Karcher, F., Ricaud, P., and Halenka, T.: Modeling the present and future impact of aviation on climate: an AOGCM approach with online coupled chemistry, Atmos. Chem. Phys., 13, 10027–10048, doi:10.5194/acp-13-10027-2013, 2013.

Huszar, P., Halenka, T., Belda, M., Zak, M., Sindelarova, K., and Miksovsky, J.: Regional climate model assessment of the urban land-surface forcing over central Europe, Atmos. Chem. Phys., 14, 12393–12413, doi:10.5194/acp-14-12393-2014, 2014.

Im, U. and Kanakidou, M.: Impacts of East Mediterranean megacity emissions on air quality, Atmos. Chem. Phys., 12, 6335–6355, doi:10.5194/acp-12-6335-2012, 2012.

Im, U., Poupkou, A., Incecik, S., Markakis, K., Kindap, T., Unal, A., Melas, D., Yenigun, O., Topcu, O., Odman, M. T., Tayanc, M., and Guler, M.: The impact of anthropogenic and biogenic emissions on surface ozone concentrations in Istanbul, Sci. Total Environ., 409, 1255–1265, doi:10.1016/j.scitotenv.2010.12.026, 2011a.

Im, U., Markakis, K., Poupkou, A., Melas, D., Unal, A., Gerasopoulos, E., Daskalakis, N., Kindap, T., and Kanakidou, M.: The impact of temperature changes on summer time ozone and its precursors in the Eastern Mediterranean, Atmos. Chem. Phys., 11, 3847–3864, doi:10.5194/acp-11-3847-2011, 2011b.

Juda-Rezler, K., Reizer, M., Huszar, P., Krueger, B., Zanis, P., Syrakov, D., Katragkou, E., Trapp, W., Melas, D., Chervenkov, H., Tegoulias, I., and Halenka, T.: Modelling the effects of climate change on air quality over central and Eastern Europe: concept, evaluation and projections, Clim. Res., 53, 179–203, doi:10.3354/cr01072, 2012.

Kanakidou, M., Mihalopoulos, N., Kindap, T., Im, U., Vrekoussis, M., Gerasopoulos, E., Dermitzaki, E., Unal, A., Kocak, M., Markakis, K., Melas, D., Kouvarakis, G., Youssef, A. F., Richter, A., Hatzianastassiou, N., Hilboll, A., Ebojie, F., von Savigny, C., Ladstaetter-Weissenmayer, A., Burrows, J., and Moubasher, H.: Megacities as hot spots of air pollution in the East Mediterranean, Atmos. Environ., 45, 1223–1235, 2011.

Katragkou, E., Zanis, P., Tegoulias, I., Melas, D., Kioutsioukis, I., Krüger, B. C., Huszar, P., Halenka, T., and Rauscher, S.: Decadal regional air quality simulations over Europe in present climate: near surface ozone sensitivity to external meteorological forcing, Atmos. Chem. Phys., 10, 11805–11821, doi:10.5194/acp-10-11805-2010, 2010.

Kiehl, J., Hack, J., Bonan, G., Boville, B., Breigleb, B., Williamson, D., and Rasch, P.: Description of the NCAR Community Climate Model (CCM3), National Center for Atmospheric Research Tech Note NCAR/TN-420 + STR, NCAR, Boulder, CO, 1996.

Kuenen, J., Denier van der Gon, H., Visschedijk, A., van der Brugh, H., Finardi, S., Radice, P., d'Allura, A., Beevers, S., Theloke, J., Uzbasich, M., Honor, C., and Perrussel, O.: A Base Year (2005) MEGAPOLI European Gridded Emission Inventory (Final Version), Deliverable D1.6, MEGAPOLI Scientific Report 10-17, MEGAPOLI-20-REP-2010-10, TNO Built Environment and Geosciences, Utrecht, the Netherlands, p. 39, 2010.

Kuhn, M., Builtjes, P. J. H., Poppe, D., Simpson, D., Stockwell, W. R., Andersson-Skold, Y., Baart, A., Das, M., Fiedler, F., Hov, Kirchner, F., Makar, P. A., Milford, J. B., Roemer, M. G. M., Ruhnke, R., Strand, A., Vogel, B., and Vogel, H.: Intercomparison of the gas-phase chemistry in several chemistry and transport models, Atmos. Environ., 32, 693–709, 1998.

Kuhn, U., Ganzeveld, L., Thielmann, A., Dindorf, T., Schebeske, G., Welling, M., Sciare, J., Roberts, G., Meixner, F. X., Kesselmeier, J., Lelieveld, J., Kolle, O., Ciccioli, P., Lloyd, J., Trentmann, J., Artaxo, P., and Andreae, M. O.: Impact of Manaus City on the Amazon Green Ocean atmosphere: ozone production, precursor sensitivity and aerosol load, Atmos. Chem. Phys., 10, 9251–9282, doi:10.5194/acp-10-9251-2010, 2010.

Lawrence, M. G., Butler, T. M., Steinkamp, J., Gurjar, B. R., and Lelieveld, J.: Regional pollution potentials of megacities and other major population centers, Atmos. Chem. Phys., 7, 3969–3987, doi:10.5194/acp-7-3969-2007, 2007.

Lee, S.-H., Kim, S.-W., Angevine, W. M., Bianco, L., McKeen, S. A., Senff, C. J., Trainer, M., Tucker, S. C., and Zamora, R. J.: Evaluation of urban surface parameterizations in the WRF model using measurements during the Texas Air Quality Study 2006 field campaign, Atmos. Chem. Phys., 11, 2127–2143, doi:10.5194/acp-11-2127-2011, 2011.

Lin, X., Roussel, P. B., Laszlo, S., Taylor, R., Melo, O. T., Shepson, P. B., Hastie, D. R., and Niki, H.: Impact of Toronto urban emissions on ozone levels downwind, Atmos. Environ., 30, 2177–2193, 1996.

Lin, Y.-C., Cheng, M.-T., Lin, W.-H., Lan, Y.-Y., and Tsuang, B.-J.: Causes of the elevated nitrate aerosol levels during episodic days in Taichung urban area, Taiwan, Atmos. Environ., 44, 1632–1640, doi:10.1016/j.atmosenv.2010.01.039, 2010.

Markakis, K., Valari, M., Perrussel, O., Sanchez, O., and Honore, C.: Climate-forced air-quality modeling at the urban scale: sensitivity to model resolution, emissions and meteorology, Atmos. Chem. Phys., 15, 7703–7723, doi:10.5194/acp-15-7703-2015, 2015.

Martin, S. T., Hung, H.-M., Park, R. J., Jacob, D. J., Spurr, R. J. D., Chance, K. V., and Chin, M.: Effects of the physical state of tropospheric ammonium-sulfate-nitrate particles on global aerosol direct radiative forcing, Atmos. Chem. Phys., 4, 183–214, doi:10.5194/acp-4-183-2004, 2004.

McMeeking, G. R., Kreidenweis, S. M., Carrico, C., Lee, T., Collett Jr., J. L., and Malm, W. C.: Observations of smoke-influenced aerosol during the Yosemite Aerosol Characterization Study: size distributions and chemical composition, J. Geophys. Res., 110, D09206, doi:10.1029/2004JD005389, 2005.

Molina, L. T., Madronich, S., Gaffney, J. S., Apel, E., de Foy, B., Fast, J., Ferrare, R., Herndon, S., Jimenez, J. L., Lamb, B., Osornio-Vargas, A. R., Russell, P., Schauer, J. J., Stevens, P. S., Volkamer, R., and Zavala, M.: An overview of the MILAGRO 2006 Campaign: Mexico City emissions and their transport and transformation, Atmos. Chem. Phys., 10, 8697–8760, doi:10.5194/acp-10-8697-2010, 2010.

Myhre, G., Grini, A., and Metzger, S.: Modelling of nitrate and ammonium-containing aerosols in presence of sea salt, Atmos. Chem. Phys., 6, 4809–4821, doi:10.5194/acp-6-4809-2006, 2006.

Nenes, A., Pandis, S. N., and Pilinis, C.: ISORROPIA: a new thermodynamic equilibrium model for multiphase multicomponent inorganic aerosols, Aquat. Geochem., 4, 123–152, 1998.

O'Brien, J. J.: A note on the vertical structure of the eddy exchange coefficient in the planetary boundary layer, J. Atmos. Sci., 27, 1213–1215, 1970.

Offenberg, J. H. and Baker, J. E.: Aerosol size distributions of elemental and organic carbon in urban and over-water atmospheres, Atmos. Environ., 34, 1509–1517, doi:10.1016/S1352-2310(99)00412-4, 2000.

Oleson, K. W., Bonan, J. B., Feddema, J., Vertenstein, M., and Grimmond, C. S. B.: An urban parameterization for a global climate model, Part I: Formulation and evaluation of two cities, J. Appl. Meteorol. Clim., 47, 1038–1060, 2008.

Pal, J. S., Small, E. E., and Eltahir, E. A. B.: Simulation of regional scale water and energy budgets: representation of subgrid cloud and precipitation processes within RegCM, J. Geophys. Res., 105, 29579–29594, 2000.

Paredes-Miranda, G., Arnott, W. P., Jimenez, J. L., Aiken, A. C., Gaffney, J. S., and Marley, N. A.: Primary and secondary contributions to aerosol light scattering and absorption in Mexico City during the MILAGRO 2006 campaign, Atmos. Chem. Phys., 9, 3721–3730, doi:10.5194/acp-9-3721-2009, 2009.

Poupkou, A., Symeonidis, P., Lisaridis, I., Melas, D., Ziomas, I., Yay, O. D., and Balis, D.: Effects of anthropogenic emission sources on maximum ozone concentrations over Greece, Atmos. Res., 89, 374–381, 2008.

Samara, C., Voutsa, D., Kouras, A., Eleftheriadis, K., Maggos, T., Saraga, D., and Petrakakis, M.: Organic and elemental carbon associated to PM_{10} and $PM_{2.5}$ at urban sites of northern Greece, Environ. Sci. Pollut. R., 21, 1769–1785, 2014.

Sarwar, G., Luecken, D., Yarwood, G., Whitten, G. Z., and Carter, W. P. L.: Impact of an updated carbon bond mechanism on predictions from the CMAQ modeling system: preliminary assessment, J. Appl. Meteorol. Clim., 47, 3–14, 2008.

Schaap, M., van Loon, M., ten Brink, H. M., Dentener, F. J., and Builtjes, P. J. H.: Secondary inorganic aerosol simulations for Europe with special attention to nitrate, Atmos. Chem. Phys., 4, 857–874, doi:10.5194/acp-4-857-2004, 2004.

Seinfeld, J. H. and Pandis, S. N.: Atmospheric Chemistry and Physics: From Air Pollution to Climate Change, J. Wiley, New York, 1998.

Sillman, S.: The relation between ozone, NO_x and hydrocarbons in urban and polluted rural environments, Millenial Review series, Atmos. Environ., 33, 1821–1845, 1999.

Simmons, A. J., Willett, K. M., Jones, P. D., Thorne, P. W., and Dee, D. P.: Low-frequency variations in surface atmospheric humidity, temperature and precipitation: inferences from reanalyses and monthly gridded observational datasets, J. Geophys. Res., 115, D01110, doi:10.1029/2009JD012442, 2010.

Simpson, D., Yttri, K. E., Klimont, Z., Kupiainen, K., Caseiro, A., Gelencser, A., Pio, C., Puxbaum, H., and Legrand, M.: Modeling carbonaceous aerosol over Europe: analysis of the CARBOSOL and EMEP EC/OC campaigns, J. Geophys. Res., 112, D23S14, doi:10.1029/2006JD008158, 2007.

Skyllakou, K., Murphy, B. N., Megaritis, A. G., Fountoukis, C., and Pandis, S. N.: Contributions of local and regional sources to fine PM in the megacity of Paris, Atmos. Chem. Phys., 14, 2343–2352, doi:10.5194/acp-14-2343-2014, 2014.

Streets, D. G. and Waldhoff, S. T.: Present and future emissions of air pollutants in China: SO_2, NO_x, and CO, Atmos. Environ., 34, 363–374, 2000.

Stock, Z. S., Russo, M. R., Butler, T. M., Archibald, A. T., Lawrence, M. G., Telford, P. J., Abraham, N. L., and Pyle, J. A.: Modelling the impact of megacities on local, regional and global tropospheric ozone and the deposition of nitrogen species, Atmos. Chem. Phys., 13, 12215–12231, doi:10.5194/acp-13-12215-2013, 2013.

Thunis, P., Rouil, L., Cuvelier, C., Stern, R., Kerschbaumer, A., Bessagnet, B., Schaap, M., Builtjes, P., Tarrason, L., Douros, J., Moussiopoulos, N., Pirovano, G., and Bedogni, M.: Analysis of model responses to emission-reduction scenarios within the CityDelta project, Atmos. Environ., 41, 208–220, doi:10.1016/j.atmosenv.2006.09.001, 2007.

Timothy, M. and Lawrence, M. G.: The influence of megacities on global atmospheric chemistry: a modeling study, Environ. Chem., 6, 219–225, doi:10.1071/EN08110, 2009.

Wang, T., Ding, A., Gao, J., and Wu, W. S.: Strong ozone production in urban plumes from Beijing, China, Geophys. Res. Lett., 33, L21806, doi:10.1029/2006GL027689, 2006.

Wang, T., Li, S., Shen, Y., Deng, J., and Xie, M.: Investigations on direct and indirect effect of nitrate on temperature and precipitation in China using a regional climate chemistry modeling system, J. Geophys. Res., 115, D00K26, doi:10.1029/2009JD013264, 2010.

Winiwarter, W. and Zueger, J.: Pannonisches Ozonprojekt, Teilprojekt Emissionen, Endbericht, Report OEFZS-A-3817, Austrian Research Center, Seibersdorf, 1996.

Xue, L. K., Wang, T., Gao, J., Ding, A. J., Zhou, X. H., Blake, D. R., Wang, X. F., Saunders, S. M., Fan, S. J., Zuo, H. C., Zhang, Q. Z., and Wang, W. X.: Ground-level ozone in four Chinese cities: precursors, regional transport and heterogeneous processes, Atmos. Chem. Phys., 14, 13175–13188, doi:10.5194/acp-14-13175-2014, 2014.

Yttri, K. E., Aas, W., Bjerke, A., Cape, J. N., Cavalli, F., Ceburnis, D., Dye, C., Emblico, L., Facchini, M. C., Forster, C., Hanssen, J. E., Hansson, H. C., Jennings, S. G., Maenhaut, W., Putaud, J. P., and Tørseth, K.: Elemental and organic carbon in PM_{10}: a one year measurement campaign within the European Monitoring and Evaluation Programme EMEP, Atmos. Chem. Phys., 7, 5711–5725, doi:10.5194/acp-7-5711-2007, 2007.

Zanis, P., Katragkou, E., Tegoulias, I., Poupkou, A., Melas, D., Huszar, P., and Giorgi, F.: Evaluation of near surface ozone in air quality simulations forced by a regional climate model over Europe for the period 1991–2000, Atmos. Environ., 45, 6489–6500, doi:10.1016/j.atmosenv.2011.09.001, 2011.

Zhang, Q. J., Beekmann, M., Freney, E., Sellegri, K., Pichon, J. M., Schwarzenboeck, A., Colomb, A., Bourrianne, T., Michoud, V., and Borbon, A.: Formation of secondary organic aerosol in the Paris pollution plume and its impact on surrounding regions, Atmos. Chem. Phys., 15, 13973–13992, doi:10.5194/acp-15-13973-2015, 2015.